1

NFMI: Near Field Magnetic Induction Based Communication

Amitangshu Pal and Krishna Kant Computer and Information Sciences, Temple University, Philadelphia, PA 19122 E-mail:{amitangshu.pal,kkant}@temple.edu

Abstract—Near Field Magnetic Induction (NFMI) based communication is an emerging technology that promises several advantages over the traditional radio frequency (RF) communication including low energy use, ability to work reliably in a variety of difficult propagation media (e.g., water, non-ferromagnetic metals, underground, tissue media of fresh produce & meats, etc.), and low leakage possibility because of fast decay. Furthermore, since the MI technology is useful for efficient power transfer as well, it provides the possibility of passive tagging as well. In this paper, we provide a technical overview of NFMI technology and its potential for several applications in RF challenged environments. We also lay out a number of challenges with NFMI technology and its use in various applications.

Index Terms—Magnetic Induction Communications, IoT, Channel Modeling, Underground communication, Underwater communication

I. INTRODUCTION

The ongoing IoT based automation is expected to transform many activities and processes that make a city or community tick. Smart sensing and short-range wireless communications form the bedrock for building sophisticated automation services. Radio frequency (RF) based communications (e.g., Bluetooth, WiFi) are well established and work extremely well in open, uncluttered environments. However, increasingly the communications needs involve environments with characteristics that make RF communications difficult - these include presence of aqueous or plant/animal tissue media which cause high signal absorption, metallic clutter that causes diffraction or shielding of the signals, or underground operation that results in an extremely complex communications channel. Reducing absorption by choosing lower frequencies helps in attenuation [1], [2], but needs bigger antennas, which introduces the problem of undesirable size and potentially severe interference with nearby radios. Also, the power consumption of RF radios is generally quite high. When localization is important, narrow-band RF technologies only provide an accuracy of a few meters, which may be inadequate [3].

Ultrasound is another well established technology that works well in aqueous and underground media, but requires larger size radios and higher power consumption, but still cannot operate in a cluttered environment. Visible light communication (VLC) is an excellent technology for line-of-sight communications through transparent media, but its performance deteriorates in presence of obstacles.

This work was supported by NSF grants under award numbers CNS-1744187 and CNS-1844944.

Because of these limitations, we focus on the emerging Near Field Magnetic Induction (NFMI or simply MI) based communication. MI communication is based on the principle of resonant inductive coupling (RIC) between two matched coils, each forming an LC circuit with the same resonance frequency. MI communication (MIC) modulates the magnetic field and forms the basis for near field communications (NFC) between MI devices. Such communication can be made purely magnetic by blocking the electric field (e.g., via an Aluminium foil) and therefore will not suffer from the usual fading and diffraction associated with the electric field. Due to these advantages, MI communication has been studied for some RF-challenged environments such as underwater [4], underground [5], and Body Area Networks [6], and some commercial products are available, such as audio headphones by NXP [7] and RuBee MI tags useful in product labeling [8].

In this paper we provide a detailed overview of the NFMI technology and communications, and discuss its research challenges and applicability to short-range wireless communication needs in the emerging IoT infrastructure. Although there are some survey articles in the literature that cover the use of magnetic induction in the context of various applications, such as underground communication [9], underwater communication [10], bio-medical applications [11] etc., a comprehensive discussion of the NFMI technology and applications is not available in the current literature. We provide such a coverage in this paper and consider the applicability and challenges of NFMI communication in food logistics, automated asset tracking, inventory control, and smart retailing. We also survey some available NFMI devices and prototypes, which are sparse in the other surveys.

The outline of the paper is as follows. Section II briefly discusses both NFMI, traditional RF/ultrasound short-range communications technologies, and VLC and shows comparison between them. Section III discusses the theoretical background of magnetic induction and MI communication. Section IV briefly describes some commercial and experimental implementations of NFMI communications technologies. Section V reviews some recent advances in the NFMI technology. Section VI discusses several communications applications involving challenging environments where the MI technology is attractive. This section also discusses how NFMI can coexist and combined with RF communication in different application scenarios. Section VII discusses several research challenges of enabling and enhancing NFMI communications. The paper is concluded in section VIII.

TABLE I COMPARISON OF NFMI AGAINST OTHER TECHNOLOGIES [12], [13]

Standard	NFMI	NFC	Bluetooth	ZigBee	Ultrasonic	VLC
Frequency	13.5 MHz [14] 131 [8] & 2–2.5 kHz [15]	13.5MHz	2.4 GHz	2.4 GHz 868-915 MHz	470 kHz	430–790 THz
Data Rate (Kb/s)	596	106-848	230-3000	20 (@868 MHz) 40 (@915 MHz) 250 (@2.4 GHz)	0.50	100 Mbps to multiple Gbps [16]
Range	2-3 m (@13.5 MHz) [17] 10's of m (@131 kHz) [8] 30 m (@2.5 kHz) [15]	≤ 10 cm	100 m or more	100 m	5cm [18] 20 cm [20]	≈ 300 m [19]
Modulation	D8PSK	ASK	GFSK/DSSS	BPSK/O-QPSK	BPSK/QPSK	OOK/PM/ OFDMA/CSK [16]
Peak current	1.35 mA [12] 18 mA (FreeLinc) [14]	50 mA	12.5 mA	30 mA	3.4 mA/Tx-mode [20] 9.1 mA/Rx-mode [20]	No product available

II. SHORT-RANGE WIRELESS COMMUNICATIONS

In this section, we briefly discuss characteristics of short-range wireless communications technologies, including radio frequency (RF), Ultrasound, Visible light communication, and MI based technologies. Table I provides a compact comparison between these technologies.

A. Short Range RF Technologies

Radio Frequency (RF) based communications are ubiquitous both for long range and short range communications. The applications considered in this paper are largely those that require communication over a rather limited range – from $\sim 1 \text{m}$ for body area networks to at most $\sim 100 \text{m}$ in smart agriculture. Therefore, we shall focus largely on short range RF technologies such as Bluetooth (BT), its variants such as low energy BlueTooth (BLE) and Zigbee.

Bluetooth is an IEEE standard technology operating in the 2.4GHz ISM band and design to communicate among a few devices in a personal area networks (PANs) [21]–[24]. It works in a master-slave architecture where one master device can connect to up to seven devices to form a *piconet*. To minimize the effect of interference with other devices, Bluetooth uses frequency hopping scheme by switching the carrier in between a set of frequency channels. Bluetooth can provide a communication range of tens or hundreds of meters, while can achieve a peak data rate of 3 Mbps. BlueTooth Low Energy (BLE or BTLE) is a slightly modified version of BT with short connection times and the device largely remains in the sleep mode [25], [26].

Zigbee is another technology similar to BlueTooth, designed to be lower power and lower speed than BT [27]–[30]. It uses the same 2.4 GHz ISM band and has 16 channels within this frequency band. It can achieve a data rate of 250 kpbs. Typical communication range of Zigbee devices is 10 meters to 100 meters. These devices can be connected together through point–to-point, mesh or start topology, using direct sequence spread spectrum (DSSS). RF based NFC (Near Field Communication) is also another relevant technology, although it is designed for very small distance operation [31], [32].

These communications are well established and work extremely well in open, uncluttered environments. However, increasingly the communications needs involve environments with characteristics that make RF communications difficult

- these include presence of aqueous or plant/animal tissue media which cause high signal absorption, metallic clutter that causes diffraction or shielding of the signals, or underground/underwater operation that results in an extremely complex communications channel. Reducing absorption by choosing lower frequencies helps in attenuation [1], but needs bigger antennas, which introduces the problem on undesirable size and potentially severe interference with nearby radios. Because of this reason BLE devices cannot be deeply implanted within human body.

RF devices coexist with several other devices around that use Bluetooth, WiFi, ZigBee, cordless phones and microwave at the ISM 2.4 GHz band. Because of this reason the RF devices can experience high interference with the other devices using ISM band. Also, the power consumption of RF radios is generally quite high which reduces the working hours of the such devices.

B. Ultrasound Communications

Another technology of interest for challenging environments is Ultrasound communications (or USC) which is based on the propagation of high frequency pressure waves through the media. Ultrasound propagation is heavily studied in underwater environments where it can be used for very low-data rate (at most a few hundred bits/sec) communications over hundreds of meters [33]–[35]. The current state of USC communications is discussed in a survey article [36] and the channel characterization in [37]. This type of communication is focused on achieving long distance rather than low power. The use of USC for body communications networks is explored in [18], [20]. Note that the numbers quoted for ultrasound in Table I are those for body area networks (small membranes). Lower frequencies and larger antennas can, of course, provide larger ranges, but at the cost of much higher power consumption.

C. Visible Light Communications

Visible light communication (VLC) has been standardized by IEEE in 2011 in the form of IEEE 802.15.7 and can achieve 100 Mb/sec or higher transmission rate for line-of-sight communications in clear media. The lack of penetration of VLC through most objects and walls however does provide opportunities for reducing interference and avoiding the problem of communication leakage.

Several survey articles have recently appeared on VLC [16], [38], [39]. In [38] the authors have discussed the physical layer techniques such as modulation, circuit design in the context of VLC, whereas the authors in [16] have studied different networking aspects such as sensing and medium access protocols of VLC. various applications of VLC are reported in [39].

Owing to its low attenuation in water, VLC has also shown promise in achieving high-speed underwater wireless optical communication (UWOC) links spanning up to hundreds of meters (≈ 300 m) [19]. UWOC is studied extensively in several recent survey articles [19], [40], [41]. In pure water the light absorption is minimum at 400–500 nm of the visible spectrum, however, such absorption characteristics change based on the amount of phyto-plankton species and dissolved organic matters in the sea water. Other than absorption, underwater scattering due to density fluctuations, organic and inorganic large particles also impacts the performance of UWOC. Also, the performance of VLC greatly deteriorates in presence of obstacles such as marine species. Overall, VLC is unusable for underground communication, implantable, intra/on-body communications, and many other important applications.

D. NFMI Communications

NFMI is a near-field communication technology (NFC) and thus it is intended to operate over a small range. This range is dependent on the frequency f (or wavelength λ), with $\lambda/2\pi f$ defining the near field limit. As discussed later, the magnetic field energy also decays quite fast (as r^{-6} with distance r), which further limits its range.

In spite of its limited range, NFMI has several desirable properties as compared to the short range RF technologies like Bluetooth. Compared to RF, NFMI-based communication has better penetration performance (i.e., low absorption) as the magnetic permeability of most nonferrous materials commonly in use is very similar to that of air. This includes aqueous media and tissue (e.g., human body, fresh produce, meat, etc.), which are high absorbent of RF. Even the austenitic stainless steel has permeability of close to 1 [42], and thus does not affect MI communications. This is demonstrated by tests done by DoE where a MI radio is kept inside a sealed stainless steel drum and one outside [43]. Furthermore, a sheet of mild steel or other forms of iron placed close to a NFMI radio essentially act like a mirror and can strengthen the signal [44]. According to the available information [45], [46], NFMI can be much more power efficient than RF, although definitive comparisons are difficult to find.

Also NFMI communication does not cause interference to other wireless networks like WiFi and BLE. Because of its short range, the same frequency can be reused for other NFMI communication. Thus in an overcrowded place using NFMI based PAN is more efficient that BLE. Fig. 1(b) illustrates the effect of frequency reuse of NFMI communication in a dense, crowded environment.

Recognizing the potential of MI communications, IEEE finalized the 1902.1 standard in 2009 that specifies a near-field MI communication protocol called *RuBee* operating at low

frequency range of 30-900 KHz [47]. Its purpose is to support low data rate applications with coin-size batteries lasting 5-10 years.

For short-range use, a popular operating frequency for NFMI is 13.56 MHz which has the near-field limit of 3.7 m and a range of 1-2 m. In this frequency band, it achieves a data rate of 400 kbps per frequency channel. There can be up to 10 frequency channels, where each channel can be subdivided further into 10 sub-channels using time division multiplexing [45]. At the lower frequency of 130 kHz (used by the IEEE RuBee standard for NFMI, discussed later), the NFMI range extends upto few tens of meter, although the achievable data rate also goes down.

E. Safety and Security of Various Technologies

As NFMI works in the low-frequency band, it significantly reduces the RF absorption by the biological tissues. The amount of RF absorption in human body is often measured by the Specific absorption rate (SAR), which is the power absorbed per mass of tissue and has units of watts per kilogram (W/kg). In United States, FCC requires that the mobile phones to have a SAR limit at or below 1.6 W/kg. Similarly the European Union has made the SAR limit to be 2 W/kg. The emissions by the NFMI is far less than this specified limit. RuBee produces 40 nano watts of RF power as compared to 4 watts for UHF RFID systems, i.e. RuBee produces about 1 quadrillion (15 zeros) less RF power than RFID [48]. As the magnetic signals are not affected in the aqueous and tissue medium, NFMI works well in deeply implanted medical devices. Because of these advantages US Food and Drug Administration (FDA) has approved NFMI as a communications technology for wireless healthcare [45]. FDA has also approved RuBee as an Non Significant Risk (NSR) technology as it has no human safety risks [48]. As mentioned in [48] RuBee is also safe near pacemakers and Implantable Cardioverter Defibrillators (ICDs).

The RF far-field signals can be intercepted and decrypted at a large distance. Because of this reason NSA has restricted the use of Bluetooth in the armed forces [45], [49]. In the context of body area networks as well the use of RF devices like Bluetooth has raised serious concerns. Bluetooth equipped implantable defibrillators, insulin pumps and infusion pumps are all been hacked [45]. In an August 29, 2017 directive, the FDA has urged anyone with pacemakers developed by Abbott (formerly St. Jude Medical) to consult their healthcare providers about a software update to address cyber-security vulnerabilities identified [50]. The agency said that due to this vulnerabilities about 465,000 radio frequency-enabled Accent, Anthem, Accent MRI, Accent ST, Assurity and Allure devices may be in danger. Researchers at IOActive have also discovered that Segway hoverboards can be hacked or locked, which may cause the riders to fall off in their mid-ride [49].

In contrast, because of the rapid decay of $1/r^6$ at distance r (or 60 dB/decade), the NFMI signal can be well contained in small region which can make NFMI communications much more secure. For example, in the context of NFMI based body area network operating at 13.56 MHz, NFMI will create a



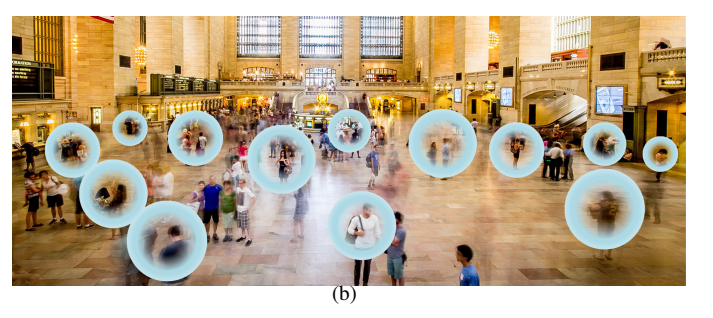


Fig. 1. (a) A magnetic bubble around an user's PAN. (b) This small bubbles ensure a significant amount of spatial reuse of the same frequency in a crowed area.

wireless *bubble* around the user as shown in Fig. 1(a). Within this bubble the devices can communicate reliably. However, the communication is invisible outside this range and thus adds a high level of security [51].

III. NFMI PRINCIPLES OF OPERATION

A. Resonant Circuits and Magnetic Induction

An RLC circuit consists of a resistor, an inductor, and a capacitor, connected in series or in parallel. Such a circuit shows resonance if the capacitive and inductive reactances (denoted X_C and X_L respectively) are equal in magnitude and hence cancel out. Since $X_C = -1/(j\omega)$ and $X_L = j\omega$ where $\omega = 2\pi f$ is the angular frequency, the resonance occurs when $\omega_T = 1/\sqrt{LC}$, and the overall impedance becomes purely resistive.

An important performance indicators of an RLC circuit is the *quality factor* Q, defined as the ratio of the energy stored in the circuit to the energy dissipated by the circuit [52], [53]. It is merely the ratio of reactance and resistance, and is given by $Q=1/\omega_rRC$). The quality factor is also defined as the frequency-to-bandwidth ratio of the resonator, i.e. $Q=\omega_r/\Delta\omega_r$ where $\Delta\omega_r$ is the resonance width, i.e. the bandwidth over which the power is greater than half the power at the resonant frequency.

Magnetic induction based communication involves two RLC coils with the same resonant frequency. Due to mutual inductance between the two coils, denoted M, a time varying voltage V_1 (and corresponding current I_1) induces a current I_2 in the receiving coil. If the resistor, inductor, and capacitor values of the two coils are (R_1, L_1, C_1) and (R_2, L_2, C_2) respectively, then from Kirchoff's laws, it is easy to conclude that $I_2 = -\frac{j\omega_r M}{R_2} I_1$. M is often expressed in terms of coupling coefficient κ between the coils, defined as $\kappa = M/\sqrt{L_1 L_2}$. Thus P_1 and P_2 are the transmitted and received power respectively, then the power transfer ratio is given by [53]

$$\frac{P_2}{P_1} = \frac{\omega_r^2 M^2 R_1 R_2}{R_1^2 R_2^2} = \kappa^2 Q_1 Q_2 \tag{1}$$

where Q_1 and Q_2 are the quality factors of the transmit and receive coils respectively. Thus, the power transfer is proportional to the coupling coefficient and the quality factors of the transceiver coils.

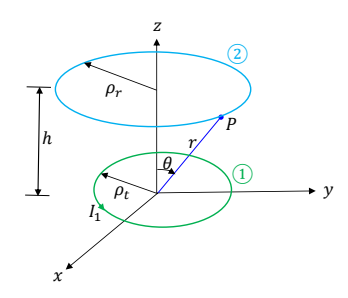


Fig. 2. Illustration of mutual inductance between two coplanar coils.

B. Mutual Inductance in between two coils

Consider two coplanar coils ① and ② in Fig. 2 with radii ρ_t and ρ_r respectively where coil ① carries a current I_1 . We assume that the coils are aligned so that the line connecting their centers is perpendicular to the coils. We can consider this line as the z (vertical) axis. Consider a point P located on the second coil at distance r and angle θ releative to the z-axis. Then the magnetic vector potential at P of coil ② due to coil ① is given by [54]:

$$\mathbf{A}_{1} = \frac{\mu I_{1} \pi \rho_{t}^{2} \sin \theta}{4 \pi r^{2}} \mathbf{a}_{\phi} = \frac{\mu I_{1} \rho_{t}^{2} \rho_{r}}{4 \left(h^{2} + \rho_{r}^{2}\right)^{3/2}} \mathbf{a}_{\phi} \approx \frac{\mu I_{1} \rho_{t}^{2} \rho_{r}}{4 h^{3}} \mathbf{a}_{\phi}$$
(2

where the approximation assumes that $h >> \rho_r$. Then the magnetic flux at coil ②, denoted Ψ_{12} , is obtained by integrating \mathbf{A}_1 around all points on coil ②, which amounts to simple multiplication by $2\pi\rho_r$. If the coils have K_1 and K_2 turns respectively, the magnetic flux increases proportionately. Furthermore, by definition, the mutual inductance M_{12} is simply Ψ_{12}/I_1 . Since the mutual inductance is reciprocal, $M_{12}=M_{21}$, we have:

$$M_{12} = M_{21} = \frac{\mu \pi K_1 K_2 \rho_t^2 \rho_r^2}{2h^3}$$
 (3)

The expression of mutual inductance is more complex of the coils are not aligned. Let us assume that the relative angles between them and the line segment connecting their centers are β_t and β_r respectively. Then the mutual inductance between them, because of current I_t flowing through the transmit coil, is given by [55]–[57]

$$M_{t \to r} = M_{r \to t} \approx \frac{\mu \pi K_t K_r \rho_t^2 \rho_r^2}{2h^3} \left| \cos \beta_t \cos \beta_r - \frac{1}{2} \sin \beta_t \sin \beta_r \right|$$

The induced AC current in the receiver coil, denoted I_r , is proportional to the rate of change of the magnetic flux

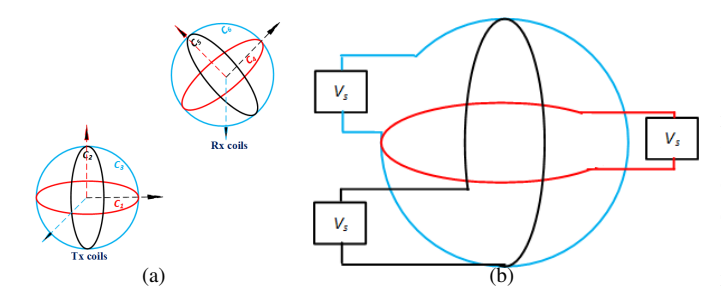


Fig. 3. Arrangement of a 3D coils in two configurations.

according to Lenz's Law, i.e., $I_r \propto M_{t \to r} f$ where f is the operating frequency. That is, the induced current increases linearly with the operating frequency. The induced current also goes down rapidly with distance r (as r^{-3}). Since the power is proportional to I_r^2 , the induced power decays as r^{-6} , which is much faster than the decay for RF. (RF power goes down as r^{-2} for free space [58], but generally faster in city environment). The very rapid decay of the induced power with distance makes the MI technology inherently a small range technology, and this effect is usually more limiting than the near field requirement of $r < \lambda/(2\pi)$. The area of transmit and receive coils (proportional to ρ_t^2 and ρ_r^2 respectively) and the number of turns $(K_t \text{ and } K_r)$ directly influence the mutual inductance and hence the induced current. Increasing the range requires bigger coils and more turns, both of which may be undesirable in applications where small size is required. The frequency and the transmit coil current directly increase the induced current, and hence the overall power consumption (bad) and the range (good).

C. Isotropic Magnetic Induction

It is seen from equation (4) that when $\beta_t = \beta_r = 0$, the coils become coplanar, and thus equation (4) reduces to equation

(3). The mutual inductance decreases with increasing β_t and β_r and becomes zero when the coils are orthogonal. Thus, if a strongly directional coupling is undesirable, one could use multiple orthogonal coils. For example, an almost isotropic field can be obtained by using 3 concentric but orthogonal coils as shown in Fig. 3. The three coils can be excited either using a single source (Fig. 3(a)) or using 3 separate sources (Fig. 3(b)) [59]. In either case, the orthogonality avoids interferences between different dimensions. However, due to finite thickness of the coil wire, a concentric 3-D coil "ball" is mechanically challenging and the field may not precisely isotropic.

To develop the equations for a 3D coils, let us start with a 1D coil located at the origin in Fig. 2, and consider an observation point located at point P which is at a distance r away from the origin. Then the magnetic field generated at the observation point $P(r, \theta, \phi)$ due to the current flowing in the z-axis (with magnitude I_z) is given by [55], [56]

$$\mathbf{h}_r^z = \frac{jk\rho^2 \mathbb{N} I_z \cos\theta}{2r^2} \left[1 + \frac{1}{jkr} \right] e^{-jkr} \hat{r}$$
 (5)

$$\mathbf{h}_{\theta}^{z} = \frac{-k^{2} \rho^{2} \mathbb{N} I_{z} \sin \theta}{4r} \left[1 + \frac{1}{jkr} - \frac{1}{(kr)^{2}} \right] e^{-jkr} \hat{\theta}$$
 (6)

$$\mathbf{h}_{\phi}^{z} = 0 \tag{7}$$

where $j=\sqrt{-1}$, ω is the angular frequency, $\rho_t=\rho_r=\rho$ is the coil radius, and $K_t=K_r=\mathbb{N}$ is the number of turns of the magnetic coil. With μ as the magnetic permeability of the medium, and ε as its electrical permittivity, the parameter k, often known as the wave number is defined as $k=\omega\sqrt{\mu\varepsilon}$.

Similarly, the corresponding fields by an unidirectional coil while the current is flowing in the x and y axis can also be generated. The resultant magnetic field at P due to the 3 unidirectional coils (which results in a tri-directional coil) is given in equation(8)-(10) [55].

$$\mathbf{h}_r^{3D} = \frac{jk\rho^2 \mathbb{N}}{2r^2} \left(I_x \cos\phi \sin\theta + I_y \sin\phi \sin\theta + I_z \cos\theta \right) \left[1 + \frac{1}{jkr} \right] e^{-jkr} \hat{r}$$
(8)

$$\mathbf{h}_{\theta}^{3D} = \frac{k^2 \rho^2 \mathbb{N}}{4r} \left(I_x \cos\phi \cos\theta + I_y \sin\phi \cos\theta - I_z \sin\theta \right) \left[1 + \frac{1}{jkr} - \frac{1}{(kr)^2} \right] e^{-jkr} \hat{\theta}$$
(9)

$$\mathbf{h}_{\phi}^{3D} = \frac{-k^2 \rho^2 \mathbb{N}}{4r} \left(I_x \sin\phi - I_y \cos\phi \right) \left[1 + \frac{1}{jkr} - \frac{1}{(kr)^2} \right] e^{-jkr} \hat{\phi}$$

$$\tag{10}$$

Comparing equations (8)-(10) against (5)-(7) we can observe that the magnetic field due to a unidirectional coil is highly directional, whereas the tri-directional coil exhibits a near-isotropic radiation. For example in equation(5) \mathbf{h}_r^z becomes zero when $\theta = \frac{\pi}{2}$. However, as \mathbf{h}_r^{3D} has both $\sin\theta$ and $\cos\theta$ components, it is never zero for any values of θ . Because of the same reason \mathbf{h}_{θ}^z becomes zero when $\theta = 0$, whereas, \mathbf{h}_{θ}^{3D} is non-zero for any values of θ . Similarly, \mathbf{h}_{ϕ}^{3D} is always non-zero for any values of ϕ . Intuitively in a tri-directional coil, if one coil's signal is minimized, then other coil's signal is maximized, thus the total magnetic field is never zero at the observation point.

D. Penetration of MI Through the Media

In the above we have shown that the MI signal power goes down as r^{-6} with distance r. In addition, one must also consider the so called *skin-effect* which affects all electromagnetic transmissions. Skin-effect is largely relevant for materials that show high conductivity. It is well-known that high-frequency signal transmission through copper wires shows the skin-effect, in that the signal current travels largely close to the surface of the wire, rather than deep inside. The signal intensity inside the wire material goes down exponentially, which has prompted the traditional definition of skin-depth as the distance over which the signal power goes down to

1/e of the original power (or by about 8.7 dB). Except at extremely high frequencies, the skin-depth can be expressed by the following simple equation [60]

$$\delta = \sqrt{\frac{2}{\omega\mu\sigma}}\tag{11}$$

where μ is the magnetic permeability, σ is the conductivity of the material (or, the inverse of resistivity), and ω is the angular frequency. Because of the large permeability, the skin-depth is extremely small for ferromagnetic materials such as iron; which is another way of saying that such materials form an effective shield against electro-magnetic signals.

As already mentioned, most materials in nature are not ferromagnetic and thus $\mu \approx \mu_0 = 1.25e^{-6}$ Henry/m. The electrical conductivity of the air is rather poor; for example, air with typical amounts of CO_2 and water vapor has conductivity in the range of $1.0e^{-5}$ in the units of per (ohm-meter) or Siemans/m. Thus in the air, the skin-depth can be 100's of meters with frequencies in the range of tens of MHz. In such cases, the normal attenuation mechanism (e.g., r^{-2} for RF) dominates. However, skin-depth may become limiting for MI propagation in challenging environments with high conductivity. For example, much of the fresh food has a large amounts of water and minerals, that could raise the conductivity significantly, but the short-distance communications required in this environment are still not limited by skin-effect.

Sea-water has conductivity of 5.0 Siemans/m, which can make the skin-effect to shrink to less than a meter. It is important to note here that since the skin-effect only considers a 8.7db signal attenuation, the corresponding range is much less than the distance over which receiver can work reliably. Overall, the signal attenuation is a product of both skin-effect and the normal attenuation discussed above. Note that unlike the normal MI communication range which increases with frequency (see section III.B), the skin-depth actually goes down with frequency. This results in the interesting phenomenon where the best signal transfer happens in a narrow frequency range [60].

Fig. 4 shows the skin-depth of different underground and underwater materials at different frequencies [60]. We choose three frequencies, 2.5 kHz, 131 kHz and 13.56 MHz for studying the skin-depths; 2.5 kHz is used in reference [15] for using in underground mines, whereas 131 kHz and 13.56 MHz are used for RuBee tags [8] and FreeLinc [14] devices respectively. From Fig. 4 we can observe that at 2.5 kHz the magnetic field penetrates deeply into most of the materials and rocks, whereas the penetration ability decreases with the increase in the operating frequency, which can be explained from equation (11). Materials like Calcite, Quartz, Petroleum have higher skin-depth, because of their low conductivity. At 13.56 MHz the skin-depth of drinking water is less than 10 meters, and even lower for sea water and saline water. At 2.5 kHz and 131 kHz also the sea water and saline water have lower skin-depth than drinking water, because of higher conductivity due to the salinity level.

Another useful concept is the radius of the sphere, say d, around a transmitter such that the signal attenuates to the level of the noise and thus becomes difficult to detect reliably. This

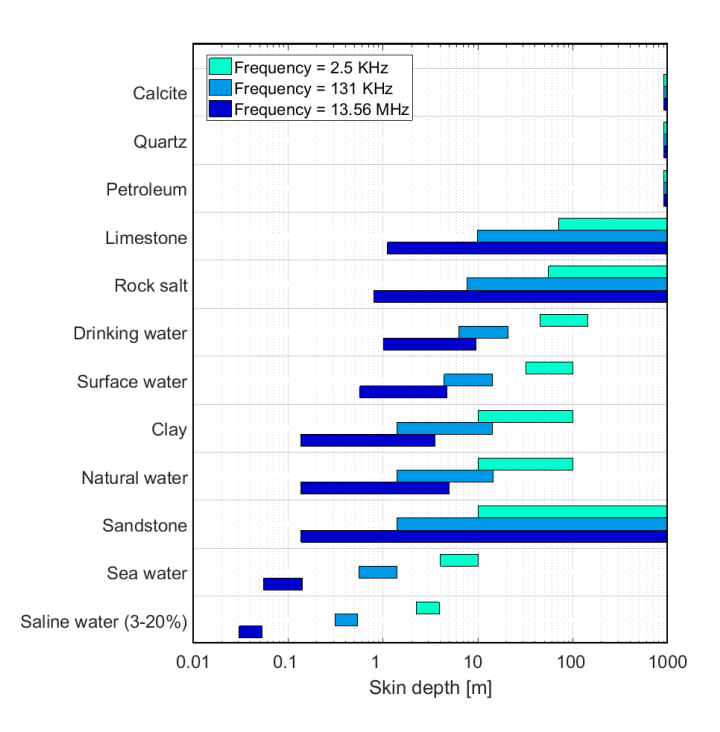


Fig. 4. Skin-depth of different underground and underwater materials at different frequencies. The data and codes are obtained from [60], [61]. The bars are showing the range of skin-depths that are obtained due to a range of values of the available parameters, such as conductivity, permittivity etc.



Fig. 5. Methods of images, where (a) a current carrying coil placed on a magnetic substrate can be represented equivalently by (b) the coil and its mirror image with respect to the substrate plain.

can be considered as a *bubble* around the transmitter and delimits the zone in which the signals can be overheard by an eavesdropper. Obviously, the radius of the communication bubble depends on the sensitivity of the receiver [62], The channel capacity C at the edge of the bubble using the Shannon-Hartley theorem is given by

$$C = B_f f_r \log_2 (1 + \text{SNR}) = B_f f_r \log_2 2 = B_f f_r$$
 (12)

where B_f is the 3dB fractional bandwidth of this near field communication system, and Q is the quality factor of the transceivers. Now B_f can be expressed as [62], [63]

$$B_f = \frac{B}{f_r} = \frac{0.664f_r}{Q} \quad \Longrightarrow \quad C = \frac{0.664f_r}{Q} \tag{13}$$

where B is the 3dB bandwidth. Thus the capacity at the edge of the bubble is proportional to the resonant frequency. Also the capacity if inversely proportional to the quality factor of the transceivers, thus increasing the quality factor does not automatically lead to higher capacity at the edge of the bubble.

E. Effect of Ferromagnetic Materials

We first explore the effect of a ferromagnetic plate on a current carrying coil. Consider a current carrying conductor carrying a current I is placed parallel to a magnetic substrate

with $\mu > 1$, as shown in Fig. 5(a). Let us assume that the substrate is at z=0, and the coil is at a distance of z_0 from the surface. Also assume that z_0 is small as compared to the thickness of the substrate. To consider the effect of the substrate, it can be considered as a semi-infinite planar slab with zero conductivity. A current current carrying conductor with a spatial current density distribution J(x,y,z) will generate a mirror image J' within the slab, which is given by [64], [65]

$$J' = \frac{\mu - 1}{\mu + 1} J_{\parallel}(x, y, -z) \qquad J'_{\perp} = -\frac{\mu - 1}{\mu + 1} J_{\perp}(x, y, -z) \tag{14}$$

where J_{\parallel} and J_{\perp} is the current density parallel and perpendicular to the substrate. If the coil is fully parallel to the substrate, then $J_{\perp}=0$. Thus an equivalent arrangement is shown in Fig. 5(b) where a mirror image of the coil will be found at $-z_0$, carrying a current of $\frac{\mu-1}{\mu+1}I$. The current density is additive to the coil current, thus placing a magnetic substrate parallel to the coil will enhance the magnetic flux and field strength in the region of interest.

From these results, one would expect that irregular shaped ferromagnetic material, including a cluttered environment consisting of many small ferromagnetic parts will tend to diffract the signal and thus push it towards greater isotropicity. Thus MI communications can work well in industrial IoT settings. Experimentally, we have also established that MI communications are not affected by static magnets [17].

IV. SOME PRACTICAL NFMI IMPLEMENTATIONS

A. Commercial NFMI devices

1) NXP NxH22xx NFMI Products: NXP NxH2280/81/61 products are ultra-low-power single chip solutions that are optimized for high quality wireless audio and data streaming using NFMI technology. These NxH22xx products are human body compatible that can penetrate through human tissues with low absorption rate. Several such devices can communicate inside the magnetic bubble around the human body, whereas outside the bubble the magnetic field is greatly attenuated. NxH22xx operates at 10.6 MHz. The real current draw of NxH22xx products is as low as 1.35 mA at 1.2 V [12]. An NXP NxH22xx NFMI chip with coil antenna is illustrated in Fig. 6(a). The chip has a dimension of 10.4 mm² with an induction coil antenna of 2 mm × 6 mm, which is small enough to fit into hearing devices. These devices can achieve an audio bandwidth more than 20 kHz over a distance of about 20 cm.

2) Freelinc NFMI devices: The Freelinc radios operate on 13.56MHz, with a current consumption of approximately 18 mA. Fig. 6 show the Freelinc transmitter board with 3-axis magnetic coils that provide near-isotropic communication environment. Two of these three coils are wrapped around a ferrite-core whereas the third one is an air-core coil, which are shown in Fig. 6(b) and Fig. 6(c) respectively. The ferrite-core coils have a diameter of < 5 mm with 9 turns, whereas the air-core one is an \sim 46 mm \times 66 mm rectangular coil. The Freelinc receiver board is only equipped with an air-core rectangular coil. The Freelinc devices can communicate within a transmission distance of around 2 meters, with a datarate of 9.6 kbps or 57.6 kbps.

3) RuBee tags from Visible Assets: Visible Assets Inc has introduced RuBee tags operating below 450 kHz (typically at 131 kHz) [8]. At 131 KHz the wavelength is of 2,289 meters, thus the near field conditions occur for up to a few hundreds of meter. Typically RuBee tags operate upto few tens of meter. Generally, RuBee tags are small devices (with a small coil) that can be attached to assets, but the RuBee readers contain a large loop antenna (LA) with 2 loops of 14 SWG multi-strand insulated copper wire, enclosed in carbon fiber tubes [66]. These tags have IP addresses, subnet addresses, MAC addresses and 256 bytes of static memory. The RuBee protocol is limited to 1200 baud, whereas the packet size is limited tens to hundreds of bytes [67]. The tags can be about the size of a postage stamp as shown in Fig. 6, but can be of larger form factors as well.

B. NFMI Experimental Prototypes

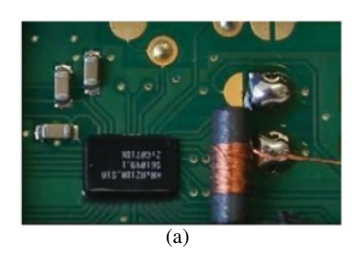
Many researchers, including us, have built experimental prototypes to study NFMI communication in various environments. In the following, we provide a brief summary of some of them. Unfortunately, much of the work in the area is fragmented and there are currently no widely available products or testbeds that researchers could use to further study the NFMI technology and its applications in a comprehensive way.

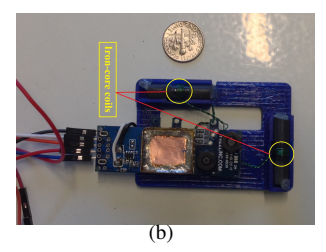
A 2.5 kHz NFMI communication system using tri-axial TX and RX coils for use in a mine is reported in [15]. To overcome the limitations of limited bitrate of MI communication, the authors have demonstrated the use of *magnetic vector modulation*, which modulates the 3-D orientation of the magnetic vector. This technique increases the bitrate by a factor over 2.5, without an increase in transmission power. In addition to that, a wide band receiver is used to receive multiple parallel streams of frequency multiplexed data. Typical communication range achieved is ~30 meters through rocks. By doing these the network latency is reduced over 4.5 times.

The same researchers have reported another system for tracking the location of burrowing underground animals, to have a view on their subterranean behavior and habits [68]. These animals are equipped with collars that record the magnetic field strengths of the received signals from transmitters placed on the surface of the burrow. This data is compressed and stored, when the animals emerge from its tunnel, the data is uploaded over a 2.4 GHz 802.15.4 link. The maximum achieved transmission rate is 11 Hz, which includes an intersignal gap of 10 ms. The antenna consumes 1.2 W of power when operational. The core of the animal tag is a Zigbit A-2 wireless sensor module with a dimension of 39 mm × 22 mm × 12 mm.

A prototype using 11 cm 3-D spherical MI coil antennas with 29 turns is reported in [59] which achieves transmission range of 40m. Their multi-coil transceiver hardware architecture is controlled by a low-power micro-controller unit (MCU). Using 3-D coils of 7.5 cm diameter at 125 KHz carrier frequency, they show a data rate of 1 kbps at over a maximum transmission range of 40m.

Microsoft Research Asia has developed a wireless proximity detection platform, named *LiveSynergy* based on magnetic





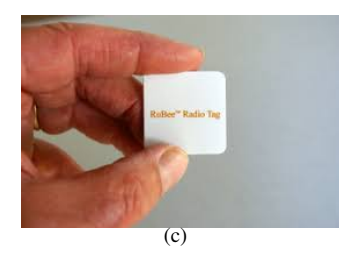


Fig. 6. Some prototype NFMI devices, (a) NXP NFMI chip with coil antenna [12] (Source: NXP Semiconductors), (b) Freelinc NFMI antennas, (c) RuBee tags [8] (Source: Visible Assets, Inc.).

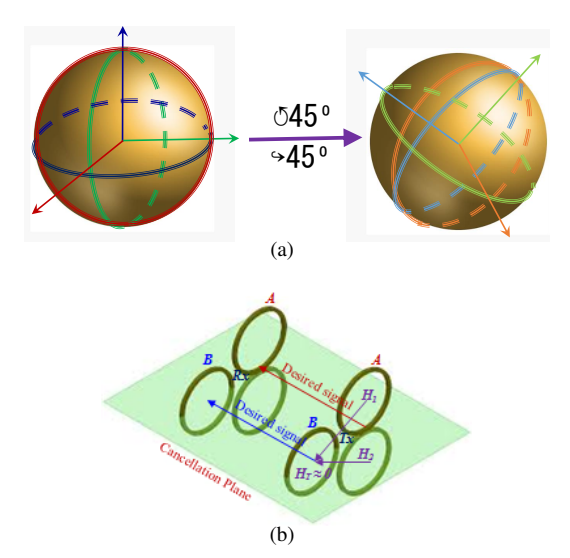


Fig. 7. Merging of two orthogonal coils for MIMO communication in (a) 3-D and (b) 1-D configurations [73].

induction to overcome the limitations of existing RF technologies [69]. Using a PCB mountable antenna of size 8cm × 1.5cm on the transmit side and a 3D magnetic coil on the receive side, they achieve a data rate of 2.73 kbps using 125 KHz carrier frequency.

We developed a MI prototype using MI TX/RX boards from Freelinc Inc that operate at 13.56 MHz. We connected each of them to a micro-controller to enable end to end packet transfer. The transceivers achieve a data rate of around 22 KBps with a current consumption of 18 mA and a distance of 2-3m.

Other than that researchers from Coastal Systems Station (CSS) and Magneto-Inductive Systems Limited (MISL) have demonstrated that MI transceivers can achieve a communication range more than 300 in meters in under sea environment [70]. Prototype for magnetic MIMO communication for capacity enhancement of the proposed NFMI communication is developed in [71]. Metamaterial-enhanced MI communication prototypes are discussed in [72], where the authors have developed a 3D sphere consists of multiple small coil antennas that enhances the magnetic field radiation.

V. RECENT ADVANCES IN MI COMMUNICATIONS

A. Enhancing MI Data Rates

The fundamental limitation of MI communication is the limited data rate. However NFMI can be used in many applications, such as transfer of personal information such as high-resolution pictures, security codes like fingerprints, multimedia

data etc. Several medical applications such as artificial retina, cochlear implants, capsule endoscopes etc. which require high-resolution data rate over 1 Mbps [71]. One of the solutions to improve the data rate of MI communication is to explore MIMO communication.

To explore MIMO communication, it is possible to integrate six coils in one module by essentially combining two sets of 3 orthogonal coils. Fig. 7(a) shows two separate coil sets where the axes are at 45 degrees relative to one another [74]. If the two are put together but operate on different channels, it should be possible to have more compact sensor modules. Ideally the axes of these two set of coils can be separated by any angle, but making them 45 degree reduce the chances of any cross-channel interference, in case the channels are fully nonorthogonal. Note that there are some mechanical challenges of putting six coils together, nevertheless, once we have a 6-coil node, we could also consider energizing all 6 coils together and thereby sending packets using these two set of coils in parallel, which results in MIMO communication and can increase the transmission capacity. As mentioned in section III, the induced current for MI communication is dependent on the carrier frequency. Thus, using multiple channels for different coil sets can result different induced current at the corresponding coil sets at the receiver. This can be compensated by using (a) different transmit power for different coil sets, or (b) by using different radius for different coil sets (which will result in one 3-D coil ball inside another one) to compensate the power difference. Ideally we can even add more number of coils, each operating on different channels to increase the data rate, however, the potential for interaction between them needs to be examined carefully.

In scenarios where we can assume that the devices are placed in identical orientations in a straight line, even 3 orthogonal coils can be used as 3 antennas for MIMO communication [75]. In fact in case of identical orientations, even multiple 1-D coils can be used for exploring MIMO communication. However, in case of 1-D coils, removing the crosstalk in between the coils is challenging. To cope with this, in [71] the authors have designed a magnetic MIMO 1-D configuration using a multi-pole loop antenna array and a circular loop antenna, which are denoted a A and B respectively in Fig. 7(b). The multi-pole loop antenna A consists of two coils, if an opposite direction current is passed through these two loops, then it will create a cancellation plane with total magnetic field $\mathbf{H_T} \approx 0$. If coil B is placed on the cancellation plane then there is not crosstalk in between the quadrupole loops and circular loops. The authors have shown through

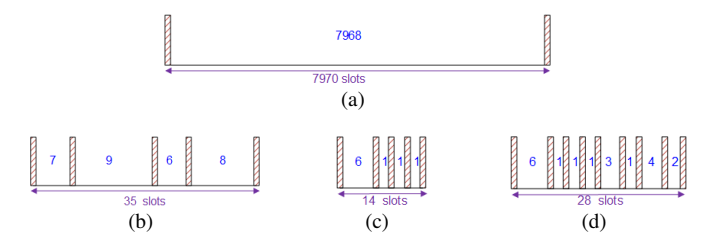


Fig. 8. CTS based communication schemes. The numbers in "blue" colors show the number of slots. The simplest version (a) can be improved by sending the digits separately (b). The scheme can be even improved further by using the sorted-CTS (c). However, this requires sending the order of the digits separately using separate signals (d).

experimental evaluations that such MIMO configuration can significantly remove the effects of crosstalk among the coils. In [76] the authors have shown that the same principle can be applied to four coils, which results in a 4×4 pyramid shaped structure.

As opposed to MIMO communication, in [15] the authors have proposed *magnetic vector modulation* where the 3-D coils are used to generate magnetic vector fields. The scheme modulates the three dimensional orientation of the magnetic vector, by controlling the phases and amplitudes of the currents in each transmitting coil. The purpose is to encode more information using the same available bandwidth and transmit power. In Binary Phase-shift keying (BPSK) data is conveyed by changing (modulating) the phase of the carrier signal, to represent values of +1 and -1. In magnetic vector modulation, by energizing each coil at a time per symbol (either with positive or negative phase), we can obtain 6 possible symbol values. By using this simple strategy, the gross bitrate is increased by a factor of $\frac{\log_2 6}{\log_2 2} = 2.58$. Notice that as a single coil is energized at a time, the overall power consumption is identical to the BPSK scheme.

B. Designing Low-Power Physical Layer Protocols

To enable the MI transceivers with ultra low-power communication framework, the authors in [74] have adopted a communication scheme through silence (CTS) [77]. The scheme relies on the time interval between two signals to convey the required information. For example if node n_1 wants to transmit 7968 to n_2 , it first sends a *start* signal (or preamble) and then waits for 7968 slots¹ before sending the stop signal, as shown in Fig. 8(a). n_2 records the interval between these two signals to derive the value being sent by n_1 . Notice that such a communication framework is much more energy efficient than typical packet based transmission. If we assume that transmitting a signal takes equivalent energy of transmitting a bit, then using CTS scheme node n_1 simply consumes energy for transmitting 2 bits. On the other hand if n_1 transmits 7968 in packet format then it sends "1111100100000" sequence of bits, i.e. spending energy for 13 bits. Thus in this scenario CTS improves the energy expenditure by more than 6 times.

However the improvement in energy comes at the cost of vastly increased delay. In the above example the receiver has to wait for 7968 slots to receive the message. To cope up with this a base system can be used, where the message is represented in a multi-digit number in that base system. For example while transmitting 7968, n_1 can transmit "7", "9", "6", "8" separately. With CTS scheme n_1 transmits signals after "7", "9", "6", "8" time slots respectively, i.e. n_2 receives the message after 35 bit time (including start and stop signals, and the intermediate 3 signals). This reduced delay comes at the cost of 3 extra intermediate bit transmissions as shown in Fig. 8(b).

To reduce the delay even further a sorted-CTS approach is proposed using differential coding based compression technique [78]. In this scheme the digits "7", "9", "6", "8" are first sorted in an increasing order, i.e. "6", "7", "8", "9". Then we code the differences of the consecutive digits, and send them along with the first digit, i.e. n_1 transmits signals after "6", "1", "1", "1" slots, i.e. n_2 receives the message after 14 bit time, which is much less than sending the actual sequence of digits. This is shown in Fig. 8(c). Notice that n_1 also needs to send the order of these digits in the original sequence, i.e. "3", "1", "4", "2". However, sending them separately will incur additional delay. For example, sending the order along with the packet-digits will result in a total delay of 28 slots as shown in Fig. 8(d). The delay is still smaller than for the pure CTS scheme, however, at the cost of 4 additional bits. Reference [74] shows that the CTS scheme can reduce the energy usage of the sensor nodes by upto 67% as opposed to typical packet based communication.

C. Localization Using MI Technology

MI-based localization schemes have been shown to be promising solutions for the indoor environment [79], underground environment [80], [81] and the pipeline environment [82]. In these approaches the sensor nodes estimate their distances from some reference points (or anchors), by using the knowledge of precise MI channel models. The most important property of magnetic localization is that obstacles such as walls, floors, and people that heavily impact the performance of typical RF communication do not alter the magnetic fields. Also MI communication is less impaired by multi-path and/or non-line-of-sight effects, which improves the localization accuracy. However, in [83] the authors have reported a number of challenges for MI positioning, including the presence of ferrous materials in the vicinity which act to bend and concentrate the flux lines, and sensitivity to user rotation and dynamics which smears the magnetic signal. The authors have overcome these challenges using signal processing and sensor fusion techniques, and have achieved positioning accuracy below 0.8 meter even in heavily distorted areas.

An interesting localization approach especially for *irrigation* application is to improve the localization accuracy using the passive sensing responses of the underground irrigation sensors. In general, the localization in underground, farming environment is challenging because the soil materials and the moisture levels vary significantly over large tracts of land. Therefore, a detailed channel model and derivation of the

¹We have assumed that the slot duration is identical to bit duration, which is also equal to the time for sending a signal.

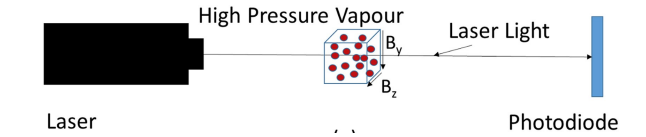


Fig. 9. Illustration of Single Laser OPM [86].

distance from the pass loss is impractical and inaccurate. To cope with this, a localization scheme for underground MI communication can be devised that runs in two phases. In the first phase few anchor nodes placed inside the field whose positions are known beforehead. Based on their positions, relative position estimate of the other nodes can be estimated using the typical localization procedures like multilateration [84], MDS-MAP [85] etc, which can be further improved by signal processing techniques as discussed in [83]. This position estimate can be further refined in the second phase by using "response of the sensor nodes corresponding to different actions". For example after watering certain portion in the field, the moisture levels of the sensor nodes in the vicinity will exhibit a change in their humidity levels. Similarly after applying fertilizer in certain sections of the field will show a change in response in the nearby sensor nodes. Thus the initial position estimate will be successively refined by observing the response of various field actions.

In [44], the authors have developed a novel mechanism for localizing shipping boxes for application #1. The purpose of such localization is not to determine a precise position estimate, but to determine which box in a pallet (or truck) has a product with quality/contamination issues. In such application in food logistics where food sensors are densely deployed, the localization is especially challenging because of the impact of mutual inductance among multiple coils and the presence of ferromagnetic materials (e.g., truck/container surface). The authors have assumed that a sensing device is placed inside each shipping boxes, and the localization scheme basically maps the sensing devices to the individual boxes. The box ID and their relative position in the truck/warehouse is recorded (manually or mechanically) during loading/unloading. By using the regular geometry of the shipping boxes and the information of their neighbor relationship, the scheme develops a neighborhood graph of boxes, denoted as G_b . It also builds a similar neighborhood graph G_s of the sensing devices based on their received signal strength from some anchors, and then exploits the geometry of G_b and G_s to estimate which sensor nodes are placed in which boxes. The authors have shown that with a small number of anchor nodes, the localization of the sensing devices can be done without any errors for boxes as small as 0.5 meter on the side. A key concern of such localization scheme is the ferromagnetic walls of the trucks that induce the eddy current from the nearby sensors and disturb the localization process. By exploiting the *image* theory (described in section III-E) the authors have argued that the presence of such walls will not disturb the localization accuracy, since they effectively "reflect" the magnetic flux and strengthen the signal, without altering the relative order of the signal strengths of the sensing devices.

D. Optically Pumped Magnetometers Based MI Communications

A different interpretation of MI communications is studied in [86], [87] where the modulated magnetic field generated by the transmitter is detected by a receiver device based on some physical phenomenon. One such detection technique is based on optical excitement of the magnetic spin of the electrons which is then modified by transmitter's magnetic field. This is a well-known technique used by optically pumped magnetometers (OPM) [86]. In the simplest setup, an OPM contains a light source (laser or discharge lamp), a high pressure vapour, and a detection system (a photo-diode) as shown in Fig. 9. The vapour is contained in small glass bulb and is made of up alkaline metal that vaporizes at low temperatures, such as Rubidium or Cesium. The polarized laser light puts the vapor atoms in a magnetically sensitive higher energy state known as optical pumping. Once the optical pumped state is established, the polarised light passes through the vapour and is detected at the photo-diode as a change in voltage. However, the optically pumped state is disrupted by the presence of a magnetic field. Thus, the output of the photo-diode, measured as a voltage, varies as a function of the magnetic field.

In more complicated setups two lasers may be used, one for optical pumping and the other for probing (or measuring the changes in the magnetic field). The probe beam wavelength is chosen to avoid pumping effect. In the presence of a magnetic field the polarisation of the probe beam rotates (by Faraday rotation) in a manner which is proportional to the magnetic state of the vapour (which in turn is a function of the magnetic field). This change in probe beam polarisation can be measured with a polarimeter. A recent article [87] describes such an OPM of size $100 \ cm^3$ using cesium vapor (stabilized around 90° C) contained in a bulb of volume $64 \ mm^3$. By using light narrowing effect, this prototype reduces the "relaxation" (i.e., loss of polarization due to bulb surface) and achieves sensitivity of $0.1 \ pT/Hz^{1/2}$ at a range of $10\mu T$.

A team from National Institute of Standards and Technology (NIST) has explored OPM for very low frequency (VLF) magnetic communication [88]. Their Rubidium based OPM can detect 1KHz modulated magnetic field with strength of 1 pT. They used a simple BPSK modulation, as it is more robust as compared to higher bit rate modulations. The achieved range was tens of meters in the indoor environment. This approach holds promise for increasing the range of NFMI communications.

E. Simultaneous Power and Data Transfer

Recently, wireless energy transfer with magnetically coupled inductive circuits, often referred to as wireless electricity (WiTricity) or Wireless Power Transfer (WPT) [89]–[91] is emerging as a viable option for recharging the sensing nodes wirelessly. Thus an interesting line of investigation is to integrate the wireless power transfer along with near-field magnetic communication, which is often referred to as *Simultaneous Wireless Information and Power Transfer (SWIPT)*. An important tradeoff in this context is the datarate (or power consumption) vs amount of energy transfer to the devices.

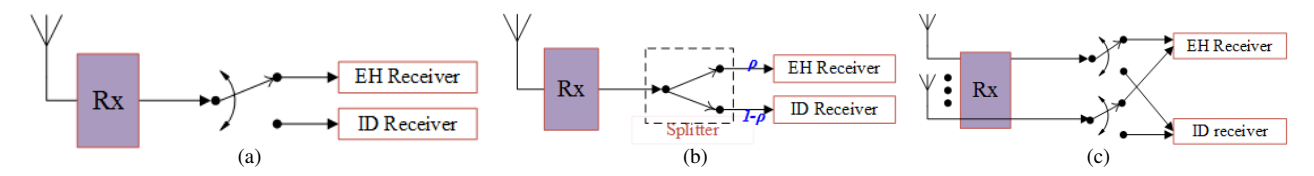


Fig. 10. SWIPT receiver of different structures (a) Time switching receiver, (b) Power splitting receiver, and (c) Antenna switching receiver.

This is because higher data transfer results in high power consumption, but ensures higher energy transfer to the devices.

In case of both power and data transfer, the SWIPT receivers need to perform two tasks: energy harvesting (EH) and information decoding (ID). Based on the structures, the SWIPT receivers can be designed in three ways [92]. When the receiver adopts *time switching*, it switches in time in between to perform harvesting and decoding tasks, as shown in Fig. 10(a). On the other hand, the *power splitting* receivers split the received signal into two streams for EH and ID, using a power splitter. Power splitting receiver is illustrated in Fig. 10(b). Power splitting receivers receiver higher design complexity than the time switching counterpart. Fig. 10(c) illustrates the *antenna switching* receivers, that switch each antenna elements in between EH and ID.

In [93] the authors have proposed an optimal power allocation strategy to maximize the transfer power efficiency of SWIPT protocol. Reference [94] has introduced a SWIPT system for reliable communication and efficient wireless powering, where the carrier frequency for power and data are assumed to be 22.4 kHz and 1.67 MHz respectively. Authors in [95] have developed a NFMI based SWIPT system for charging electric vehicles, which supports wireless powering and data transfer such as battery status, vehicle identification number (VIN) etc from vehicle to the charger.

In SWIPT architecture, canceling crosstalks in between the uplink, downlink and power transfer is important for achieving high data rate and energy transfer. In [96], [97] the authors have proposed multi-carrier systems to support separated data and power transmission. Usually the crosstalk in between the power transfer and data signals cannot be significantly reduced, even with different carrier frequencies, unless there is a reasonable spectral separation between the power and data signals [96]. To cope with this, the authors in [96] have proposed a multi-carrier crosstalk cancellation scheme using non-coherent DPSK. The authors in [98] have proposed a high-bandwidth-utilization wireless power and information transmission based on dual-mode differential phase shift keying (DDPSK). Reference [97] also proposed a multicarrier system for full duplex data communication and power transfer using inductive coupling. They have also compared an orthogonal coil geometry with a coplanar coil structure to reduce the crosstalk effect, and have shown that the latter is more robust to lateral misalignment. Similar frequency division multiplexing (FDM) based full-duplex SWIPT system has been developed in [99].

For single-carrier NFMI SWIPT architecture Load shift keying (LSK) or load modulation (LM) scheme is usually used as a popular modulation technique, which identifies the reflected impedance in the transmitter coil via the changing load impedance of the receiver coil [73]. In LSK, a high quality factor results in higher power transfer efficiency, but restricts the data rate. Because of this tradeoff, LSK is not capable of achieving high transfer efficiency along with high data rate. In [100] the authors have described a passive phase shift keying (PPSK) modulation scheme for SWIPT via a single inductive link. The PPSK scheme reverses the current phase of the secondary coil using half-period switching, which leads to increased current and thus data transfer in the primary coil [73]. Reference [101] proposed a cyclic on-off keying (COOK) modulation scheme for SWIPT that achieves both high power transfer and data rate using backscattering.

The WPT efficiency largely varies based on the multiple factors including coil size, geometry, number of turns, and most importantly the transmission distance. The technology has been largely investigated for implantable device power transfer with the range of at most a few cm, and good transfer efficiency is possible in these cases [102], [103]. For example, a very recent publication [104] shows the best case transfer of 68 mW with efficiency of 67% across 2 cm.

In addition to the range limitation, the efficiency of WPT drops significantly for either lateral or angular misalignment among the transceiver coils occur [105]. Various techniques have been studied to overcome these limitations. The authors in [106], [107] have studied an adjustable matching circuit that switches inductor and capacitor array, whereas the authors in [108] have designed a coil array to deal with the misalignment. 3-D coils structures are studied in [109]–[111] to solve the influence of the angular misalignment. The authors in [112] have presented a dual-resonant mixed coupling structure to reduce the effect of misalignment, by considering the duality property of electrical coupling and magnetic coupling.

F. Interference and Overhearing in MI Communications

In order to reduce the energy consumption or extend the battery life (in case of battery power sensing applications) of the MI devices, it is crucial to keep the electronics associated with each MI node to be dormant (in a deep sleep mode or completely unpowered) unless it needs to transmit or receive (hear) a transmission. For this, a very low power wake-up circuitry can be integrated with each coil which itself remains awake all the time. The wakeup circuit is triggered by the induced current in the coil and wakes up the radio receiver electronics only when the induced current is above some threshold. The radio transmitter appends a short preamble before transmitting the actual data packet, which is sufficiently long to wake-up the receiver circuit. The wakeup mechanism allows the radio to sleep most of the time. Due to the near-field

transmissions via the coupled magnetic field, the receiver coil can detect the MI signal without actively listening. Hence, an MI signal intended for a near-by sensor device may also be detected. This can cause severe overhearing problem (hearing transmissions destined to others) in a very dense sensor environment. In such a dense networks, interference is also a crucial issue.

For such a scheme to work, a proper scheduling of transmissions is crucial depending on the specific environment. Another complication here is that because of the short range of MI transmissions, multi-hop communication is a must at least in applications #1, #2 where we have a grid of MI radios (one per box in application #1, or one per square land tract in application #2 etc.). In addition, there will be a number of anchor nodes deployed on the periphery that act as sinks. In most scenarios, it is unlikely that the internal nodes will be able to directly communicate with the anchor nodes. Thus, multihop communication will be essential for data collection and can be handled by using well known schemes for building data-gathering tree/forest leading from each device to its nearest sink-node (e.g., [113]), but this needs to be done to minimize energy consumption. In addition, the MI waveguide method (e.g., [5], [114], [115]) and the cooperative relaying techniques (e.g., [5], [6], [116]) can be exploited to extend the transmission range and/or enhance the received signal.

For scheduling, a "conflict graph" can be constructed, i.e., which groups of nodes have a mutual overhearing problem. This can be done either based on number of hops [117] or based on the signal-to-interference-plus-noise ratio (SINR) will also be studied [118]. All nodes within a conflict set can use a TDMA based schedule. The size of the conflict set and the time constraints on the overall time required determine the viability of such a scheme.

Using multiple channels is another way to reduce the overhearing; however, this involves building in the complexity of dynamic channel selection. In [74] the authors have introduced such a multi-channel selection scheme for MI communication. In this paper the *receiver channel* of a node is its designated channel for receiving all incoming packets. In contrast, a *transmit channel* is the one to which a node switches temporarily to transmit, and is the receiver channel of the intended destination. Nodes select their receiver channels to enable distribution of traffic over multiple orthogonal channels. Since nodes listen to their receiver channels by default, interference/overhearing is limited to neighboring transmissions on a node's receiver channel only. By such dynamic channel selections the authors have shown that the overall overhearing counts is reduced by $\sim 60\%$ with 2 channels and by $\sim 80\%$ with 4 channels.

VI. NFMI APPLICATIONS AND THEIR CHALLENGES

NFMI can be competitive or preferable in several environments that involve media that is difficult for RF to traverse efficiently. In the following we discuss several such applications and point out the advantages of and challenges in using NFMI communications.

A. Application 1: Fresh Food Transportation and Distribution

Transportation and distribution (T&D) of fresh food is a huge and growing enterprise but suffers from poor efficiency (in 10-20% range [119]), and spoilage/waste of around ~12% [120]. Fresh food is also easily contaminated, and together with deteriorated fresh food is responsible for most of *Food Borne Illnesses* (FBI), and affects roughly 1 in 6 Americans (or 48 million) each year [121], [122]. Better management of fresh food T&D that reduces spoilage, tracks contamination, and increases T&D efficiency can have wide ranging societal, economic and ecological benefits. It is worth noting that better T&D can also reduce food waste at the source via better pickup scheduling and on customer end by delivering fresher food that is less likely to be tossed.

Food sensor development is currently a very active field with sensors ranging from simple to highly sophisticated ones, with functionalities including bacterial content, contamination, texture/color degradation, bruising, etc. Simple sensors are beginning to show up in packages sold to end customers, such as C₂Sense [123], FoodScan [124], Salmonella Sensing System [125] etc.

In order to automate quality sensing, suitable sensors need to be integrated with a radio for communication and inserted into each box of fresh food. Generally, each box is rather small in size, but many such boxes are often stacked into a pallet (e.g., 8x8x8) that are transported between the distribution centers. The radios would be expected to organize into a multihop communication network in order to carry all of the sensed data to a point outside the pallet.

In [44], [126] the authors have developed the overall architecture for the proposed system by considering deployment within a carrier (a truck) carrying one or more pallets of boxes with one sensor per box. The sink (or anchor) nodes are mounted on (or close to) the inner walls of the carrier. As the food boxes carry water containing products (i.e. fruits and vegetables) or meat packages, the sensor modules need to communicate via NFMI as opposed to typical radio communication does not work well in this environment. The sink nodes also communicate with sensor modules and among themselves via NFMI. A WiFi interface is also integrated in some (at least one) anchors, so that they can communicate with the "local hub", such as driver's smartphone and then on to a centralized place such as the cloud for correlation and analytics.

There are many challenges in cost effectively using MI communications in this environment. First, the sensing and radio modules must be highly rugged and energy efficient so that they can be deployed, removed and redeployed repeatedly for multiple years in product boxes. Alternately, the modules must be made very inexpensive both in sensor and radio costs and designed to be essentially "built-into" the boxes. Second, with one module per food box, the radios are very closely packed and interference among them could be a significant problem. Third, building a multi-hop communication network in a pallet that is tolerant of placement and alignment variations can be challenging.

B. Application 2: Underground Soil Monitoring

The rapid depletion in ground water levels in most parts of the world is increasing the necessity of advanced systems to use the water efficiently for irrigation. Micro-irrigation techniques can achieve this by delivering just the right amount of water to each small area of the agriculture field based on the characteristics of the soil, moisture level, and needs/condition of the plant in that area. This requires burying sensors in the ground close to the plant roots, collecting the data periodically (e.g., once a day), and doing some analytics to determine the irrigation needs [127], [128]. Another important aspect is the controlled use of fertilizers both for optimal plant growth and also to minimize waste of fertilizers, since any excess fertilizers end up in the waterways and ultimately in the oceans, causing algae blooms and other problems. Optimal fertilizer application requires automated sensing of soil nutrients like Nitrogen, Potassium, pH close to the plant

As the RF communication does not penetrate through the ground and rocks, MI technology may be appropriate in the application. Preliminary studies of the typical soil materials (rock, soil, mineral, water) show that majority of the underground materials are non-magnetic and thus have relative magnetic permeability close to free-space value [129]. This article also points out that the ferromagnetic materials are rare in nature. Similar conclusion is also pointed out in [130], [131]. Other than the permeability, the conductivity of the underground materials are also important in soil characterization. Electrical conductivity of the soil materials generates eddy current and produces out-of-phase secondary field [132]. This field superimposes with the primary field and results in distortion, which results the magnetic field to decay fast through the material. The soil conductivity is also a function of soil moisture, age of the rocks, location and local conditions etc. [130]. However at very low frequencies the eddy current due to conductivity is sufficiently low for most underground materials [132], [133].

Unlike fresh food application, this application requires a much longer range (in few tens of meters), and thus the lower frequencies (less than 1 MHz) are essential for near field communications. However, lower frequency means lower induced current, which must be compensated by making the coils bigger. Burying larger coils underground is more expensive and can be particularly challenging in agricultural fields where the farm machinery may disturb, dig up, or even chop off the coils and associated electronics. A solution is to bury them deeper but that results in weaker signal and may make the sensing close to roots more difficult.

C. Application 3: Underwater sensor networks

The applications of underwater WSNs (UWSNs) have huge potential for monitoring the health of marine aquaculture, underwater pollution detection and control, underwater habitat monitoring, climate monitoring and tracking any disturbances etc. UWSNs are also useful for oil or mining industries for oil/gas extraction, oil spills, mine detection etc. Such networks can also be useful for monitoring underwater disasters such as

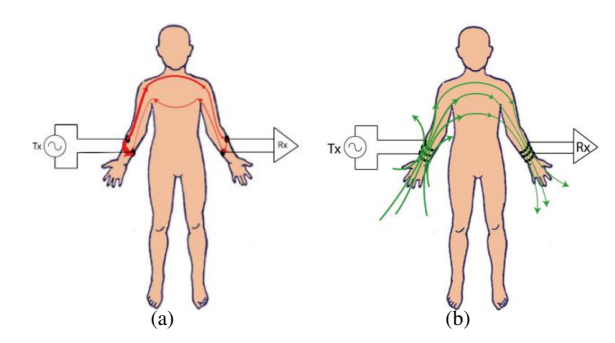


Fig. 11. Human body communication scheme (a) through electric fields, and (b) magnetic fields [139].

underwater volcanic eruptions, underwater earthquakes that results in tsunamis, floods etc. Like underground environments, RF communication is also affected in UWSNs. Acoustic communication is found as a viable option for UWSNs [34], [134]. However, the propagation delay of acoustic signals are pretty high, due to the propagation speed of 1500 m/s. Multi-path fading and Doppler effects of acoustic signals also limits the communication quality using acoustics [135]. Because of higher propagation delay and multi-path effects, acoustic signals are also affected by turbulence caused due to tidal waves and suspended sediments [136]. The acoustic communication is also adversely affected in shallow water, due to multiple reflected paths from the surface (i.e. waterair boundary) [137], [138]. As opposed to acoustics, MI communication enjoys higher propagation speed (3 \times 10⁸ m/s) and experiences negligible multi-path effects, thus exploring and using MI communications can be a suitable option for UWSNs. MI communication is expected to be less affected by turbulence and less impaired in shallow water where noise, reflectivity and multi-path propagation impair acoustic communication [138]. It is also possible to transmit MI signals across different media, i.e. across water/air or soil/air interfaces. In fact, the attenuation rate is less affected due to such interfaces, because of similar magnetic permeabilities of these media. The experiments using RuBee show that the transceivers kept inside different media (i.e. air and water) can indeed communicate successfully and the communication distance remains unaffected across media [8].

Similar to underground communication, underwater communication also requires long communication range, which can be achieved by using lower frequencies and larger coils. In addition to that, in underwater environment, the coils are needed to be placed in different altitudes, thus 3D propagation characteristics is essential. Fortunately, this can be achieved in NFMI by integrating three orthogonal coils together.

D. Application 4: Human Body Communication

Human body communication typically uses communication across human body through electric fields, known as *electric human body communication (eHBC)* [140], [141]. In such approaches, the transceivers are attached to the skin; the transmitter generates a time varying electrical signal, which induces current across the human body and is sensed by the receiver, as shown in Fig. 11(a). As the transmitted signal is

limited within the body, such communication achieves high level of security/privacy. eHBC is also resilient to interference with other devices in the vicinity. Along with that eHBC is also resilient to human body movement, postures, and can also communicate with the implants. However, the key limitation of eHBC is the rather low electrical conductivity of the human tissue medium, which results in large path loss.

To cope up with the low conductivity of the human tissue, magnetic human body communication (mHBC) is introduced in [139]. In mHBC, coils are attached/wrapped around different parts of the body, and can communicate by generating/receiving magnetic energy, which is illustrated in Fig. 11(b). Low conductivity coupled with magnetic permeability close to that for the air implies that magnetic signals should propagate better through the human body. Reference [139] has used an operating frequency of 21 MHz which results in the near-field range of 2.3 meter and limits the propagation of such magnetic signal outside the human body. mHBC also enjoys similar benefits of eHBC, such as privacy/security, low interference, higher spatial reuse etc. Because of these reasons, mHBC is also used in commercial headsets by Freelinc/NXP for ear-to-ear audio communication through the human head. mHBC will also be useful for military usages to eliminate cables between a soldier's onbody devices. In fact mHBC can be used along with eHBC for higher security and privacy; as eHBC propagation is strictly limited within a human's body, it can be used for implementing the security protocols such as key exchanges, whereas the actual data transfer and communication can be implemented using mHBC for better signal quality and higher data rate.

Near field magnetic induction can also be used for cochlear implants that are widely used to restore the auditory senses in the hearing-impaired people [142]. A cochlear implant consists of an external unit and an implanted stimulator unit. The external unit is worn behind the ear and consists of a microphone, speech processor, and a transmitter. The auditory signal processed from the external unit is transmitted wirelessly to the implanted unit, which electrically stimulates the remaining auditory nerve fibers in the cochlea. Similar magnetic coupling based communication/power transfer can also be applied to cardiac, cortical, retinal, peripheral, spinal, and optogenetic implants as reported in [142].

They key challenges of mHBC is to build MI coils with small form factor, and with low power consumption. To maintain the information privacy, short transmission range is adequate in HBC; thus, the use of high frequency MI signals (typically in MHz range) are appropriate for mHBC. Another key challenge is interference in scenarios where a group of people come very close to each other. The level of interference is still expected to be lower than the RF due to faster decay of the MI signals.

E. Application 5: IoT Supported Retailing

Retailing is generally a people intensive industry including those needed as cashiers, shelvers, inventory managers, customer helpers, etc. However, the Industry 4.0 related automation, electronic product labeling, and a suitable IoT based

sensing/communications infrastructure can reduce this considerably. In fact, given the low margins and stiff competition, the future of retail must necessarily automate the more routine functions such as shelving of products and checkout. The vision of the cashier-less retailing is that a customer would enter the retail store, collect all the desired products, and simply walk out of a specially sensored exit that identifies the products and charges customer's account. Such a system not only saves retailers money, it also eliminates the queues in cashier lines that customers generally do not like [143].

There are already some such efforts on the retail market, the best known being *Amazon Go* [144] where the items chosen by customers are checked out via a camera based surveillance and corresponding analytics to identify the products. A similar effort is Toshiba's *Touchless Commerce* [145] that lets customer checkout 10 or less items. However these vision based technologies are inherently limited to line of sight operation and suffer from privacy concerns and high costs of vision based product identification. Thus mechanisms using some sort of electronic product labels that can be read directly are quite attractive.

RuBee tags along with a larger RuBee reader can provide a reasonable solution here. We assume that the readers are attached to the retail entrance and exit, thus whenever a customer enters the store, his identity (i.e. customer ID) is read by this readers. We assume that each customer carries a card that has a RuBee tag with an unique customer ID. Similarly each shopping item also carries a MI tag printed on the package, which carries its ID along with other shopping related information (such as cost, manufacturer ID, date-of-expiry etc.). At the exit, the reader reads the customer ID along with the item tags the customer carries, and the subsequent amount is charged into the customers card. The process is illustrated in Fig. 12.

However, the large-scale, practical implementation of MI tags in retailing comes with a number of challenges. These tags need to be inexpensive enough to be installed and printed on every product package. At the same time, their power consumption needs to be extremely low so that the circuitry can be charged/activated through back-scattering from the RuBee readers. When the reader activates and transmits a query to the tags, all tags in close vicinity will wake-up their circuitry and respond to the query with the product details. The responses from multiple such tags could also interfere with each others transmission, but could be handled by a typical ALOHA based technique: the tag needs the capability to detect if its transmission is experiencing collision and if so it needs to backoff with a random delay.

The above mechanism can be extended to a more fine-grain tracking of customer behavior in terms of putting a certain item in the cart and then exchanging it with a similar item (e.g, a cheaper store brand item, or one with more or less features) or simply taking the item out after considering its purchase. This requires a few small readers embedded in the cart itself. Online tracking of products picked up temporarily and actually bought allows the retailer to gain more insight about the preferences of individual customers, and can help them with customer specific advertising or coupon distribution (See Fig. 12(b)).

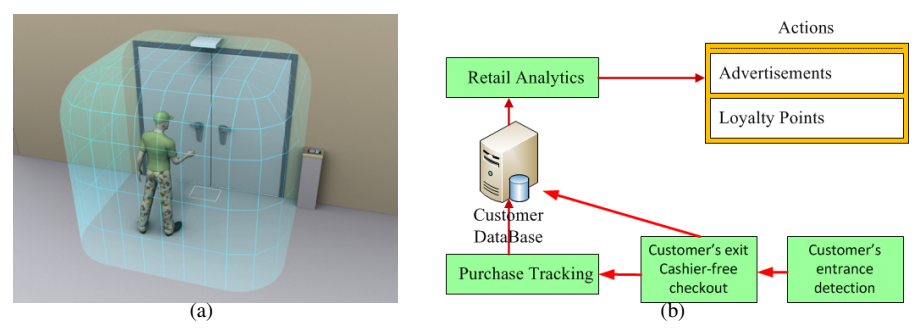


Fig. 12. (a) Customer identification at the retail entrance [8] (Source: Visible Assets, Inc.). (b) Cashier-free retailing architecture.

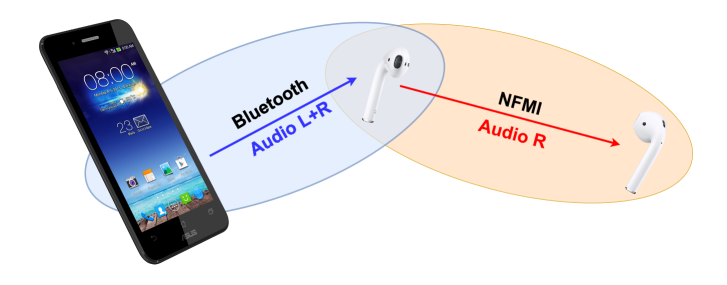


Fig. 13. Combined BLE and NFMI based communication [146].

E-tailers like Amazon already does product recommendations based on analytics of the purchase and browsing data. This is a bit harder for physical retailers, since they only have the purchase data. The tracking of physical browsing of products (in term of what products are picked up) can fill this gap.

F. Other potential application areas

NFMI can also be useful for communication among devices/sensors in autonomous vehicles or between car devices and the occupants. Many noncritical automotive body domain applications, such as seat control, window lift, mirror adjustment, and light control inside a car that are now-adays controlled via field bus communication systems can be made wireless [147]-[149]. As many of such automotive communication environment needs some sensors to be submerged in a liquid, or substantially surrounded by metallic structures, RF communication may be problematic. In fact, for in-vehicle communication (where devices are placed inside vehicle compartments) RF experiences high loss, as studied in [150], [151]. Thus depending on the sensor locations in an inside vehicle, automotive communication environment, some of these communication links can be replaced by NFMI, especially ones that are severely guarded by metallic structures, whereas others can use BT links.

Other than these applications, NFMI based communications is attractive for many short distance IoT applications that requires high security, human safety, low-power and operates in harsh environments/mediums such as aqueous, soil, tissue or steel. Such communication technologies can be integrated with sensors for monitoring temperature, vibration, humidity or other diagnostic purposes that are useful for various IoT applications. In fact the technology can also be used in

industrial IoT (IIoT) environment such as assembly line automation where the robotic tools need to communicate among themselves and possibly with the parts they are working with in a highly cluttered environment. Reference [8] has reported the use of RuBee tags in many such applications, such as automated asset tracking [152], secure weapon maintenance system [153], detection and security, supply chain audits, inventory control etc.

In fact NFMI can also coexist with the existing RF solutions in future IoT environments. Typical BLE applications work in a hub-and-spoke architecture. For example a smartphone/computer can work as a hub whereas the peripherals (like earpieces, mouse, keyboards etc.) connect them with the hub. As NFMI can reach 3-10 feet easily at 13.56 MHz, such applications can use NFMI instead of BLE. For example the system shown in Fig. 13 is an example of a wireless music/audio streaming system introduced by NXP [146]. In Fig. 13 the left earbud is equipped with both BLE and NFMI, whereas the right one is only equipped with an NFMI radio. In such a music streaming system, the smartphone sends an audio stream to the left earbud using BLE, which then forwards the audio stream to the right earbud using NFMI. Using BLE in between the earbuds is also feasible but will result in RF absorption into the brain and thus packet drops, constant re-pairing, increased power consumption etc. and thus is replaced by NFMI. NFMI also experiences less audio latency as compared to BT based audio streaming [154]. In Fig. 13 the BLE link can be replaced by another NFMI link, if the future smartphones are equipped with NFMI based communications.

More generally, NFMI will augment BLE with emerging chipsets equipped with both technologies. If the devices are equipped with dual technologies, then NFMI may be used for secured application or at the time of security/handshaking, whereas BLE can be used for exchanging regular communication packets. The other possibility is to opportunistically use and switch these two technologies: for example the devices can switch to NFMI mode for running few applications when the RF channels are overloaded in a crowded scenario and vice versa. Such opportunistic use of BLE and NFMI is also possible in Fig. 13 if the smartphones are equipped with both of these technologies so that the link between the smartphone and the left earbud can opportunistically switch between BLE and NFMI.

Notice that very low cost (perhaps disposable) radios are

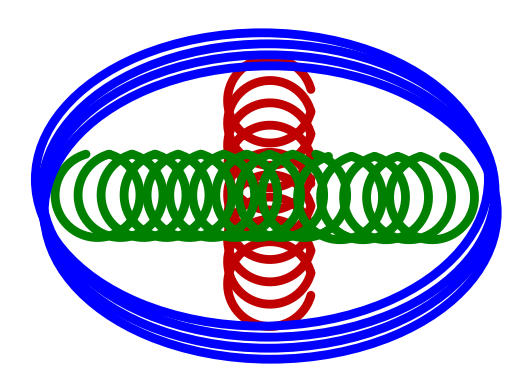


Fig. 14. Illustration of an almost planar, isotropic antenna with 3 orthogonal coils.

essential for applications requiring mass deployment such as #1 and #5 where the radios need to be embedded in each end consumer level packages and discarded ultimately by the consumer. Sensors and radios typically go together as a single module, and given the costs of Silicon, it is difficult to achieve costs of 1 cent per module [155]. However, the emerging printed, flexible circuits on paper/plastic substrates can achieve low costs and at the same time can be much more environmentally friendly [155]. There is a tremendous amount of ongoing research on paper based sensors [156] and various forms of food quality sensing mechanisms [157]. Technologies such as inkjet-printed on-chip sensors and antennas on flexible substrates, multi-walled carbon nanotube based solutions are expected to realize thus miniaturization and low-cost solutions. Such miniaturized, printed circuit based solutions are currently being researched heavily [158]-[161] and will be expected to help in miniaturization, power consumption, and cost.

VII. RESEARCH CHALLENGES AND FUTURE DIRECTIONS

In spite of many recent works on NFMI communications, a significant number of challenges and open areas still remain concerning the technology. These range from coil design, protocol development to the underline physics related of magnetic communication. Below we summarize these along with some possible approaches.

Antenna design: The induced magnetic field by a NFMI coil is necessarily orthogonal to the coil, and the field strength goes down as a cosine of the angle in other directions. This means that to generate omni-directional signal, one would need 3 orthogonal coils which are ideally concentric. This is problematic since it results in 3D geometries which could be unwieldy in some applications. While RF antennas also have limited radiation pattern, the 2-D signal propagation, slow decay, and diffraction make the RF antenna design less challenging than NFMI. One option to do this is to make a (a) circular base with bigger diameter and fewer turns for one axis, whereas (b) helical coils in two other axis with smaller diameter and higher number of turns, as shown in Fig. 14. Such a structure makes it almost planar and concentric. In fact, the helical coils can also be wrapped around ferrite-cores (similar to Freelinc antennas in Fig. 6(b)) to enhance the signal strength in their orthogonal direction. A related issue is to shape the coil to achieve a specific radiation pattern, for example, to achieve the desired beam width and direction for the magnetic field so as to increase the transmission range in the desired direction. This is particularly important for intrabody applications where both the size/shape and the desired direction of transmission must be tightly controlled.

Limited transmission range/data-rate: Another issue with magnetic communication is its small transmission range (a few meters at 13.56 MHz) and much lower data rates than RF (400 Kb/sec at 13.56 MHz as opposed to a few Mb/sec). The latter can be addressed to some extent by using MIMO (multiple-input, multiple-output) techniques which essentially amounts to using multiple coils operating on different frequency channels and has been explored in the literature to a limited extent using USRP boards [162]–[164]. Increasing the range requires overcoming two limitations: (a) the need to keep the range below $\lambda/2\pi$ to maintain NFC communication, and (b) fast decay of induced signal with distance.

Problem (a) can be addressed by simply choosing a low operating frequency - for example, lowering the frequency from 13 MHz to 1.3 MHz increases the range from 3.5m to 35m, which is quite adequate for most applications. However, this frequency decrease would also decrease the induced current by a factor of 10, and to compensate for it, we would need to increase the coil diameter and/or number of turns suitably. For example, in applications with multiple receive coils and a single transmit coil, one could double the number of turns and increase the diameter by 2.236X for the transmit coil while keeping the receive coils the same. Such an increase may be reasonable for IoT applications where antennas of more than a few inch diameter can be accommodated, but not for others. Problem (b) is fundamental to NFMI and can only be addressed by installing repeaters in the path. In particular, the authors in [165] have explored a NFMI waveguide to increase the range, by putting several coils in succession coils separated by some distance and tuning them to a slightly different frequency. Although such a solution can cover longer distances, it is practically unweildy in most situations.

Optically pumped magnetometer (OPM), discussed in section V appears to be promising techniques to improve the datarate and communication range to tens of meters. OPM achieves satisfactory signal-to-noise ratio in tens of meters, however, it has the potential to be extended to hundreds of meters [88]. The technology also suffers from localization inaccuracies; the NIST team has reported the localization inaccuracy of 16 meters which is quiet high for many practical purposes. The main research direction to achieve these goals is to improve the noise suppression techniques and develop better algorithms that can accurately extract distance measurements.

Ultra-low power NFMI communication: Many applications mentioned in section VI require ultra-low power NFMI communication, such as using this technology on food packages for sensing and reporting the food quality where replacing batteries is expensive. One of the main techniques studied for ultra-low power communication is communication through silence (CTS) [74]. However, the extent of success of this scheme depends on how fast the transceiver electronics can be switched on from sleep mode or put back to sleep, which

TABLE II
SUMMARY OF CHALLENGES AND POTENTIAL DIRECTIONS OF NFMI COMMUNICATION

Challenges	Details	Possible approach
Coverage	Flat coils are most practical but have strongly	Omni-directional communication can be achieved using 3
Specific Antenna	directional radiation pattern	orthogonal coils, but the form factor (ball) very inconvenient
Design	 Induced magnetic field is created in direction that 	Need specialized antennas (e.g., helical, circular/rectangular)
	is orthogonal to the coil	base, etc.) that is both compatible with the physical limitations
	• Signal strength goes down as a cosine of the angle	of placement and provides a desired radiation pattern
	in other directions	
Longer Commu-	Traditional methods are problematic, i.e., larger di-	Optically pumped magnetometer based transmission, how-
nication Range	ameter/more turns makes antenna physically un-	ever, such technique needs to be studied further for better
	wieldy, lower frequency increases near-field range	noise suppression and better localization accuracy
	but reduces transmitted power, and repeaters at short	
	distances are undesirable	
Increased data	MI can deliver up to about 400 Kb/sec, which may	Creative Multiple-input and Multiple-out (MIMO) an-
rates	be inadequate for some short distance applications	tenna design along with channel assignment and interfer-
		ence/overhearing mitigation
		OPM based transmission
Ultra-low power	Energy availability is extremely limited in many	Fine grain power management of the electronics and antenna
communications	embedded applications of MI	to minimize power consumption during idle periods between
		transmission of symbols
Combined energy	To minimize power waste in the antenna, the com-	Tradeoff between energy efficient communication (e.g., silent
and data transfer	munication and energy transfer must be overlapped	communication) and energy transfer need
	as much as possible	

remains as the key design challenge of this scheme. The scheme also incurs higher communication latency, thus, a mixed binary/CTS transmissions might be studied for reducing delays or for carrying higher rate MI communications. The noise tolerance of such scheme also needs future research.

Combined energy and data transfer: Designing simultaneous power and data transfer protocols for low-power NFMI communication is another potential challenge to make this technology applicable especially in energy limited environments, such as communication in between multiple intra-body, implantable devices. To improve both the communication and power transfer efficiency, the communication and energy transfer must be overlapped as much as possible. Depending on the placement of the network nodes and their connectivity/vicinity, an intelligent scheduling policy needs to be adopted to achieve this goal. The design of such scheduling policies need to be adaptive and should consider several important issues including (a) the available harvesting potential for various nodes in the network and ability to send energy to other nodes, (b) the local monitoring/actuation needs of each node, (c) the communications load of the nodes (i.e., need to send data to or receive data from other nodes), and (d) the distance and relative misalignment potential of each pair of nodes and the corresponding signal attenuation and noise characteristics.

Table II summarizes the fundamental research challenges and potential research directions of NFMI communication.

VIII. CONCLUSIONS

Given the unique characteristics of NFMI communications – operability in difficult RF environments, very low power, and possibility of simultaneous power transfer – NFMI communication can be useful in several short range IoT applications involving RF challenged environments. In this article, we have explored the strengths and limitations of this technology in several such application areas. In environments requiring small form factors, MI transceivers can operate reliably for long periods with small coin batteries and yet support the range

requirements of the application, such as in body area networks. NFMI can also be used with simultaneous power transfer, thus eliminating the need of using batteries.

However, the technology also suffers from some limitations, the most important one being the limited range if the antennas and the current consumption are to be kept low. We hope that this article will evoke a greater interest in examining this technology to a wider set of emerging IoT applications and addressing the corresponding challenges.

REFERENCES

- [1] R. Jedermann, T. Pötsch, and C. Lloyd, "Communication techniques and challenges for wireless food quality monitoring," *Philosophical Transactions of the Royal Society of London A: Mathematical, Physical and Engineering Sciences*, vol. 372, no. 2017, p. 20130304, 2014.
- [2] F. A. Khan, "Sub-gigahertz wireless sensors for monitoring of food transportation," Master's thesis, University Bremen, 2015.
- [3] H. Liu, H. Darabi, P. P. Banerjee, and J. Liu, "Survey of wireless indoor positioning techniques and systems," *IEEE Trans. Systems, Man, and Cybernetics, Part C*, vol. 37, no. 6, pp. 1067–1080, 2007.
- [4] I. F. Akyildiz, P. Wang, and Z. Sun, "Realizing underwater communication through magnetic induction," *IEEE Communications Magazine*, vol. 53, no. 11, pp. 42–48, 2015.
- [5] Z. Sun and I. F. Akyildiz, "Magnetic induction communications for wireless underground sensor networks," *IEEE Transactions on Anten*nas and Propagation, vol. 58, no. 7, pp. 2426–2435, 2010.
- [6] M. Masihpour, D. Franklin, and M. Abolhasan, "Multihop relay techniques for communication range extension in near-field magnetic induction communication systems," *Journal of Networks*, vol. 8, no. 5, pp. 999–1011, 2013.
- [7] "NXP Introduces Ultra-low Power Radio Transceiver Enabling Wireless Earbuds," http://www.everythingrf.com/News/details/1399nxp-introduces-ultra-low-power-radio-transceiver-enabling-wirelessearbuds.
- [8] http://ru-bee.com/.
- [9] S. Kisseleff, I. F. Akyildiz, and W. H. Gerstacker, "Survey on advances in magnetic induction-based wireless underground sensor networks," *IEEE Internet of Things Journal*, vol. 5, no. 6, pp. 4843–4856, 2018.
- [10] Y. Li et al., "A survey of underwater magnetic induction communications: Fundamental issues, recent advances, and challenges," *IEEE Communications Surveys and Tutorials*, vol. 21, no. 3, pp. 2466–2487, 2019.
- [11] H. Kim et al., "Review of near-field wireless power and communication for biomedical applications," *IEEE Access*, vol. 5, pp. 21264–21285, 2017

- [12] "Near-field magnetic induction for wireless audio and data streaming," https://www.futureelectronics.com/resources/get-connected/2017-06/ future-electronics-near-field-magnetic-induction.
- [13] M. Ghamari, H. Arora, R. S. Sherratt, and W. Harwin, "Comparison of low-power wireless communication technologies for wearable healthmonitoring applications," in *I4CT*, 2015, pp. 1–6.
- [14] http://www.freelinc.com/.
- [15] A. Markham and N. Trigoni, "Magneto-inductive networked rescue system (miners): Taking sensor networks underground," in *IPSN*, 2012, pp. 317–328.
- [16] P. H. Pathak, X. Feng, P. Hu, and P. Mohapatra, "Visible light communication, networking, and sensing: A survey, potential and challenges," *IEEE Commun. Surv. Tutorials*, vol. 17, no. 4, pp. 2047–2077, 2015.
- [17] R. Gulati, A. Pal, and K. Kant, "Experimental evaluation of a near-field magnetic induction based communication system," in *IEEE WCNC*, 2019.
- [18] M. Li and Y. T. Kim, "Feasibility analysis on the use of ultrasonic communications for body sensor networks," *Sensors*, vol. 18, no. 12, Dec 2018.
- [19] H. M. Oubei et al., "Light based underwater wireless communications," Japanese Journal of Applied Physics, vol. 57, no. 8S2, 2018.
- [20] G. E. Santagati and T. Melodia, "Experimental evaluation of impulsive ultrasonic intra-body communications for implantable biomedical devices," *IEEE Trans. Mob. Comput.*, vol. 16, no. 2, pp. 367–380, 2017.
- [21] P. McDermott-Wells, "What is bluetooth?" *IEEE Potentials*, vol. 23, no. 5, pp. 33–35, 2005.
- [22] K. V. S. S. S. S. Sairam, N. Gunasekaran, and S. R. Redd, "Bluetooth in wireless communication," *IEEE Communications Magazine*, vol. 40, no. 6, pp. 90–96, 2002.
- [23] C. Bisdikian, "An overview of the bluetooth wireless technology," *IEEE Communications Magazine*, vol. 39, no. 12, pp. 86–94, 2001.
- [24] E. Ferro and F. Potorti, "Bluetooth and wi-fi wireless protocols: a survey and a comparison," *IEEE Wireless Communications*, vol. 12, no. 1, pp. 12–26, 2005.
- [25] K. E. Jeon, J. She, P. Soonsawad, and P. C. Ng, "Ble beacons for internet of things applications: Survey, challenges, and opportunities," *IEEE Internet of Things Journal*, vol. 5, no. 2, pp. 811–828, 2018.
- [26] S. D. Padiya and D. V. S. Gulhane, "Iot and ble beacons: Demand, challenges, requirements, and research opportunities- planning-strategy," in CSNT, 2020, pp. 125–129.
- [27] C. M. Ramya, M. Shanmugaraj, and R. Prabakaran, "Study on zigbee technology," in *International Conference on Electronics Computer Technology*, 2011, pp. 297–301.
- [28] S. Safaric and K. Malaric, "Zigbee wireless standard," in ELMAR, 2006, pp. 259–262.
- [29] W. Wang, G. He, and J. Wan, "Research on zigbee wireless communication technology," in *International Conference on Electrical and Control Engineering*, 2011, pp. 1245–1249.
- [30] Manpreet and J. Malhotra, "Zigbee technology: Current status and future scope," in *ICCCS*, 2015, pp. 163–169.
- [31] J. Ylinen, M. Koskela, L. Iso-Anttila, and P. Loula, "Near field communication network services," in *International Conference on Digital Society*, 2009, pp. 89–93.
- [32] M. Csapodi and A. Nagy, "New applications for nfc devices," in Mobile and Wireless Communications Summit, 2007, pp. 1–5.
- [33] M. Stojanovic and J. C. Preisig, "Underwater acoustic communication channels: Propagation models and statistical characterization," *IEEE Communications Magazine*, vol. 47, no. 1, pp. 84–89, 2009.
- [34] M. Stojanovic, "Underwater acoustic communications," in *IEEE Electro International*, 1995, pp. 435–440.
- [35] G. Lee et al., "Experimental results of long range underwater communication based on chirp-fh signals," in ICUFN, 2019, pp. 39–41.
- [36] F. Cañete et al., "Measurement and modeling of narrowband channels for ultrasonic underwater communications," Sensors, vol. 16, no. 2, p. 256, 2016.
- [37] F. Caete, J. Lpez-Fernndez, and C. Garca-Corrales, "Measurement and modeling of narrowband channels for ultrasonic underwater communications," *Sensors*, vol. 16, 2016.
- [38] D. Karunatilaka, F. Zafar, V. Kalavally, and R. Parthiban, "LED based indoor visible light communications: State of the art," *IEEE Commun. Surv. Tutorials*, vol. 17, no. 3, pp. 1649–1678, 2015.
- [39] N. Kumar and N. Loureno, "Led-based visible light communication system: A brief survey and investigation," *Journal of Engineering and Applied Sciences*, vol. 5, pp. 296–307, 04 2010.
- [40] C. Shen et al., "Laser-based visible light communications and underwater wireless optical communications: a device perspective," in SPIE, 2019, pp. 29 37.

- [41] G. Schirripa Spagnolo, L. Cozzella, and F. Leccese, "Underwater optical wireless communications: Overview," *Sensors*, vol. 20, no. 8, 2020.
- [42] "Magnetic properties of stainless steels," https://www.cartech.com/en/alloy-techzone/technicalinformation/technical-articles/magnetic-properties-of-stainless-steels.
- [43] R. Drayer, "Applications of current technology for continuous monitoring of spent fuel," SRNL Report SRNL-STI-2013-00342, 2013.
- [44] A. Pal and K. Kant, "Magnetic induction based sensing and localization for fresh food logistics," in *IEEE LCN*, 2017, pp. 383–391.
- [45] "Nfmi: Connectivity for the iot," https://www.linkedin.com/pulse/nfmiconnectivity-iot-michael-abrams/, 2016.
- [46] "Magnetic induction vs. rf: power benefits, drawbacks," https://www.eetimes.com/document.asp?doc_id=1225281.
- [47] IEEE, "Standard for long wavelength wireless network protocol," *IEEE Std 1902.1-2009*, pp. 1–25, 2009.
- [48] "Rubee human safety summary," http://ru-bee.com/Academy/HumanSafe/index.html.
- [49] "Why your bluetooth devices arent as secure as you think," https://www.inc.com/joseph-steinberg/are-your-bluetooth-devicessecure-maybe-not.html.
- [50] "mhealth hacking threat prompts fda to issue pacemaker recall," https://mhealthintelligence.com/news/mhealth-hacking-threat-prompts-fda-to-issue-pacemaker-recall, 2017.
- [51] "Near field magnetic induction (nfmi): Dreams of wireless hearables," http://www.audioxpress.com/article/near-field-magnetic-inductionnfmi-dreams-of-wireless-hearables.
- [52] J. I. Agbinya, Principles of Inductive Near Field Communications for Internet of Things. Wharton, TX, USA: River Publishers, 2011.
- [53] M. Masihpour, "Cooperative communication in near field magnetic induction communication systems," Ph.D. dissertation, University of Technology, Sydney, 2012.
- [54] M. Sadiku, Elements of electromagnetics. New York: Oxford University Press, 2015.
- [55] H. Guo, Z. Sun, and P. Wang, "Channel modeling of MI underwater communication using tri-directional coil antenna," in *IEEE GLOBE-COM*, 2015, pp. 1–6.
- [56] C. A. Balanis, Antenna Theory: Analysis and Design. Wiley-Interscience, 2005.
- [57] X. Tan and Z. Sun, "Environment-aware indoor localization using magnetic induction," in *IEEE GLOBECOM*, 2015, pp. 1–6.
- [58] H. T. Friis, "A note on a simple transmission formula," Proceedings of the IRE, vol. 34, no. 5, pp. 254–256, 1946.
- [59] N. Ahmed, A. Radchenko, D. Pommerenke, and Y. R. Zheng, "Design and evaluation of low-cost and energy-efficient magneto-inductive sensor nodes for wireless sensor networks," *IEEE Systems Journal*, pp. 1–10, 2018.
- [60] T. E. Abrudan, O. Kypris, N. Trigoni, and A. Markham, "Impact of rocks and minerals on underground magneto-inductive communication and localization," *IEEE Access*, vol. 4, pp. 3999–4010, 2016.
- [61] "Impact of rocks and minerals on underground magneto-inductive communication and localization," https://www.mathworks.com/ matlabcentral/fileexchange/56632-impact-of-rocks-and-minerals-onunderground-magneto-inductive-communication-and-localization?s_ tid=mwa_osa_a, 2016.
- [62] J. I. Agbinya et al., "Characteristics of the magnetic bubble 'cone of silence' in near-field magnetic induction communications terminals," *Journal of Battlefield Technology*, vol. 13, no. 1, pp. 21–25, 2010.
- [63] H. C. Jing and Y. E. Wang, "Capacity performance of an inductively coupled near field communication system," in *IEEE Antennas and Propagation Society International Symposium*, 2008, pp. 1–4.
- [64] W. A. Roshen and D. E. Turcotte, "Planar inductors on magnetic substrates," *IEEE Transactions on Magnetics*, vol. 24, no. 6, pp. 3213– 3216, 1988.
- [65] K. O'Donoghue and P. Cantillon-Murphy, "Planar magnetic shielding for use with electromagnetic tracking systems," *IEEE Transactions on Magnetics*, vol. 51, no. 2, pp. 1–12, 2015.
- [66] http://ru-bee.com/Academy/Sec/index.html.
- [67] "Ru bee rubee disadvantages and advantages," http://www.liquisearch.com/ru bee/rubee disadvantages and advantages.
- [68] A. Markham, N. Trigoni, S. A. Ellwood, and D. W. Macdonald, "Revealing the hidden lives of underground animals using magnetoinductive tracking," in *SenSys*, 2010, pp. 281–294.
- [69] X. Jiang et al., "Design and evaluation of a wireless magnetic-based proximity detection platform for indoor applications," in IPSN, 2012, pp. 221–232.

- [70] J. J. Sojdehei, P. N. Wrathall, and D. F. Dinn, "Magneto-inductive (mi) communications," in MTS/IEEE Oceans 2001. An Ocean Odyssey. Conference Proceedings (IEEE Cat. No.01CH37295), 2001, pp. 513–519.
- [71] H. Kim et al., "Near-field magnetic induction mimo communication using heterogeneous multipole loop antenna array for higher data rate transmission," *IEEE Transactions on Antennas and Propagation*, vol. 64, no. 5, pp. 1952–1962, 2016.
- [72] H. Guo, Z. Sun, and C. Zhou, "Practical design and implementation of metamaterial-enhanced magnetic induction communication," *IEEE Access*, vol. 5, pp. 17213–17229, 2017.
- [73] H. Kim et al., "Review of near-field wireless power and communication for biomedical applications," *IEEE Access*, vol. 5, pp. 21264–21285, 2017
- [74] A. Pal, R. Gulati, and K. Kant, "Towards building low power magnetic communication protocols for challenging environments," in *ICCCN*, 2019.
- [75] S. Li, Y. Sun, and W. Shi, "Capacity of magnetic-induction mimo communication for wireless underground sensor networks," *Int. J. Distrib. Sen. Netw.*, vol. 11, no. 10, 2015.
- [76] N. Tal, Y. Morag, and Y. Levron, "Magnetic induction antenna arrays for mimo and multiple-frequency communication systems," *Progress In Electromagnetics Research C*, vol. 75, pp. 55–167, 2017.
- [77] Y. Zhu and R. Sivakumar, "Challenges: Communication through silence in wireless sensor networks," in ACM MobiCom, 2005, pp. 140–147.
- [78] B. Krishnaswamy et al., "Time-elapse communication: Bacterial communication on a microfluidic chip," IEEE Trans. Communications, vol. 61, no. 12, pp. 5139–5151, 2013.
- [79] X. Tan and Z. Sun, "Environment-aware indoor localization using magnetic induction," in 2015 IEEE Global Communications Conference (GLOBECOM). IEEE, 2015, pp. 1–6.
- [80] T. E. Abrudan, Z. Xiao, A. Markham, and N. Trigoni, "Underground incrementally deployed magneto-inductive 3-d positioning network," *IEEE Trans. Geoscience and Remote Sensing*, vol. 54, no. 8, pp. 4376– 4391, 2016.
- [81] S. Lin, A. A. Alshehri, P. Wang, and I. F. Akyildiz, "Magnetic induction-based localization in randomly deployed wireless underground sensor networks," *IEEE Internet of Things Journal*, vol. 4, no. 5, pp. 1454–1465, 2017.
- [82] X. Tan, Z. Sun, and P. Wang, "On localization for magnetic induction-based wireless sensor networks in pipeline environments," in 2015 IEEE International Conference on Communications (ICC). IEEE, 2015, pp. 2780–2785.
- [83] T. E. Abrudan, Z. Xiao, A. Markham, and N. Trigoni, "Distortion rejecting magneto-inductive three-dimensional localization (magloc)," *IEEE Journal on Selected Areas in Communications*, vol. 33, no. 11, pp. 2404–2417, 2015.
- [84] N. Lasla, A. Bachir, and M. F. Younis, "Area-based vs. multilateration localization: A comparative study of estimated position error," in *IWCMC*. IEEE, 2017, pp. 1138–1143.
- [85] L. Zhang, H. Wang, Z. Hu, and D. Wang, "An enhanced distributed localization algorithm based on MDS-MAP in wireless sensor networks," iJOE, vol. 13, no. 3, pp. 27–39, 2017.
- [86] T. M. Tierney, N. Holmes, and e. Stephanie Mellor, "Optically pumped magnetometers: From quantum origins to multi-channel magnetoencephalography," *NeuroImage*, vol. 199, pp. 598 – 608, 2019. [Online]. Available: http://www.sciencedirect.com/science/article/pii/ S1053811919304550
- [87] Y. Guo, S. Wan, X. Sun, and J. Qin, "Compact, high-sensitivity atomic magnetometer utilizing the light-narrowing effect and in-phase excitation," *Appl. Opt.*, vol. 58, no. 4, pp. 734–738, Feb 2019. [Online]. Available: http://ao.osa.org/abstract.cfm?URI=ao-58-4-734
- [88] V. Gerginov, F. C. S. da Silva, and D. Howe, "Prospects for magnetic field communications and location using quantum sensors," *Review of Scientific Instruments*, vol. 88, no. 12, p. 125005, 2017. [Online]. Available: https://doi.org/10.1063/1.5003821
- [89] A. A. Eteng, S. K. A. Rahim, and C. Y. Leow, "Wireless nonradiative energy transfer: Antenna performance enhancement techniques." *IEEE Antennas and Propagation Magazine*, vol. 57, no. 3, pp. 16–22, 2015.
- [90] A. Karalis, J. D. Joannopoulos, and M. Soljacic, "Efficient wireless non-radiative mid-range energy transfer," ANNALS OF PHYSICS, vol. 323, 2006.
- [91] A. Kurs et al., "Wireless power transfer via strongly coupled magnetic resonances," Science, vol. 317, no. 5834, pp. 83–86, 2007.
- [92] S. Bi, C. K. Ho, and R. Zhang, "Wireless powered communication: opportunities and challenges," *IEEE Communications Magazine*, vol. 53, no. 4, pp. 117–125, 2015.

- [93] K. Lee and D.-H. Cho, "Simultaneous information and power transfer using magnetic resonance," *ETRI Journal*, vol. 36, no. 5, pp. 1003– 1005. 2014.
- [94] J. Wu et al., "Wireless power and data transfer via a common inductive link using frequency division multiplexing," *IEEE Transactions on Industrial Electronics*, vol. 62, no. 12, pp. 7810–7820, 2015.
- [95] C. Huang, C. Lin, and Y. Wu, "Simultaneous wireless power/data transfer for electric vehicle charging," *IEEE Transactions on Industrial Electronics*, vol. 64, no. 1, pp. 682–690, 2017.
- [96] M. Zhou, M. R. Yuce, and W. Liu, "A non-coherent dpsk data receiver with interference cancellation for dual-band transcutaneous telemetries," *IEEE Journal of Solid-State Circuits*, vol. 43, no. 9, pp. 2003–2012, 2008.
- [97] G. Simard, M. Sawan, and D. Massicotte, "High-speed oqpsk and efficient power transfer through inductive link for biomedical implants," *IEEE Transactions on Biomedical Circuits and Systems*, vol. 4, no. 3, pp. 192–200, 2010.
- [98] P. Guo et al., "High-bandwidth-utilization wireless power and information transmission based on ddpsk modulation," *IEEE Access*, vol. 7, pp. 85 560–85 572, 2019.
- [99] Y. Yao et al., "An fdm-based simultaneous wireless power and data transfer system functioning with high-rate full-duplex communication," *IEEE Transactions on Industrial Informatics*, vol. 16, no. 10, pp. 6370– 6381, 2020.
- [100] D. Cirmirakis et al., "A fast passive phase shift keying modulator for inductively coupled implanted medical devices," in 2012 Proceedings of the ESSCIRC (ESSCIRC), 2012, pp. 301–304.
- [101] S. Ha et al., "Energy recycling telemetry ic with simultaneous 11.5 mw power and 6.78 mb/s backward data delivery over a single 13.56 mhz inductive link," *IEEE Journal of Solid-State Circuits*, vol. 51, no. 11, pp. 2664–2678, 2016.
- [102] B. Lee and M. Ghovanloo, "An overview of data telemetry in inductively powered implantable biomedical devices," *IEEE Communications Magazine*, vol. 57, no. 2, pp. 74–80, 2019.
- [103] K. Peng, X. Tang, S. Mai, and Z. Wang, "A simultaneous power and downlink data transfer system with pulse phase modulation," *IEEE Transactions on Circuits and Systems II: Express Briefs*, vol. 66, no. 5, pp. 808–812, 2019.
- [104] M. Yuan et al., "Magnetic resonance-based wireless power transfer for implantable biomedical microelectronics devices," in *IEEE ISSPIT*, 2019, pp. 1–4.
- [105] K. Fotopoulou and B. W. Flynn, "Wireless power transfer in loosely coupled links: Coil misalignment model," *IEEE Transactions on Mag*netics, vol. 47, no. 2, pp. 416–430, 2011.
- [106] S. G. Lee, H. Hoang, Y. H. Choi, and F. Bien, "Efficiency improvement for magnetic resonance based wireless power transfer with axialmisalignment," *Electronics Letters*, vol. 48, no. 6, pp. 339–340, 2012.
- [107] T. Campi, S. Cruciani, F. Maradei, and M. Feliziani, "Near-field reduction in a wireless power transfer system using lcc compensation," *IEEE Transactions on Electromagnetic Compatibility*, vol. 59, no. 2, pp. 686–694, 2017.
- [108] B. Kallel, O. Kanoun, and H. Trabelsi, "Large air gap misalignment tolerable multi-coil inductive power transfer for wireless sensors," *IET Power Electronics*, vol. 9, no. 8, pp. 1768–1774, 2016.
- [109] O. Jonah, S. V. Georgakopoulos, and M. M. Tentzeris, "Orientation insensitive power transfer by magnetic resonance for mobile devices," in 2013 IEEE Wireless Power Transfer (WPT), 2013, pp. 5–8.
- [110] W. M. Ng, C. Zhang, D. Lin, and S. Y. Ron Hui, "Two- and three-dimensional omnidirectional wireless power transfer," *IEEE Transactions on Power Electronics*, vol. 29, no. 9, pp. 4470–4474, 2014.
- [111] D. Liu, H. Hu, and S. V. Georgakopoulos, "Misalignment sensitivity of strongly coupled wireless power transfer systems," *IEEE Transactions* on Power Electronics, vol. 32, no. 7, pp. 5509–5519, 2017.
- [112] T. Yu, W. Huang, and C. Yang, "Design of dual frequency mixed coupling coils of wireless power and data transfer to enhance lateral and angular misalignment tolerance," *IEEE Journal of Electromagnetics*, *RF and Microwaves in Medicine and Biology*, vol. 3, no. 3, pp. 216– 223, 2019.
- [113] Y. Wu, Z. Mao, S. Fahmy, and N. B. Shroff, "Constructing maximum-lifetime data gathering forests in sensor networks," *IEEE/ACM Transactions on Networking (TON)*, vol. 18, no. 5, pp. 1571–1584, 2010.
- [114] Z. Sun and I. F. Akyildiz, "Underground wireless communication using magnetic induction," in *IEEE International Conference on Communi*cations. IEEE, 2009, pp. 1–5.
- [115] Z. Sun and I. F. Akyildiz, "Deployment algorithms for wireless underground sensor networks using magnetic induction," in 2010 IEEE

- Global Telecommunications Conference (GLOBECOM 2010). IEEE, 2010, pp. 1–5.
- [116] M. Masihpour and J. I. Agbinya, "Cooperative relay in near field magnetic induction: A new technology for embedded medical communication systems," in 2010 Fifth International Conference on Broadband and Biomedical Communications (IB2Com). IEEE, 2010, pp. 1–6.
- [117] G. Sharma, R. R. Mazumdar, and N. B. Shroff, "On the complexity of scheduling in wireless networks," in *Proceedings of the annual inter*national conference on Mobile computing and networking (MobiCom). ACM New York, NY, USA, 2006, pp. 227–238.
- [118] P. Gupta and P. R. Kumar, "The capacity of wireless networks," Information Theory, IEEE Transactions on, vol. 46, no. 2, pp. 388–404, 2000.
- [119] B. Montreuil, "Towards a physical internet: Meeting the global logistics sustainability grand challenge," *Logistics Research*, vol. 3(2-3), pp. 71– 87, 2011.
- [120] D. Gunders, "Wasted: How america is losing up to 40 percent of its food from farm to fork to landfill," 2012.
- [121] CDC, "Estimates of foodborne illness in the united states," https://www.cdc.gov/foodborneburden/estimates-overview.html, 2016.
- [122] CDC, "Foodborne outbreak online database (food tool)," http:// wwwn.cdc.gov/foodborneoutbreaks/, 2015.
- [123] C2Sense, "C2sense," http://www.c2sense.com, accessed: March 18th, 2016.
- [124] http://www.israel21c.org/keeping-food-safe-from-farm-to-fork/.
- [125] Phys.org, "Salmonella sensing system: New approach to detecting food contamination enables real-time testing," http://phys.org/news/2013-10-salmonella-approach-food-contamination-enables.html, accessed: March 18th, 2016.
- [126] A. Pal and K. Kant, "Iot-based sensing and communication infrastructure for the fresh food supply chain," *IEEE Computer*, feb 2018.
- [127] R. J. N., T. B. C., and B. A. R., "Effect of drip irrigation and plastic mulch on yield, water use efficiency and benefit-cost ratio of pea cultivation," *Journal of the Indian Society of Soil Science*, vol. 46, no. 4, pp. 562–567, 1998.
- [128] S. von Westarp, S. Chieng, and H. Schreier, "A comparison between low-cost drip irrigation, conventional drip irrigation, and hand watering in nepal," *Agricultural Water Management*, vol. 64, no. 2, pp. 143–160, 2004.
- [129] W. Telford, L. Geldart, and R. Sheriff, Applied Geophysics. Cambridge University Press, 1990. [Online]. Available: https://books.google.co.in/books?id=Q8ogAwAAQBAJ
- [130] A. D. W. Gibson, Channel characterisation and system design for sub surface communications. University of Leeds, 2003. [Online]. Available: http://etheses.whiterose.ac.uk/4169/
- [131] I. T. Union, Electrical characteristics of the sufrace of earth, 1992.
- [132] J. Sogade et al., "Electromagnetic cave-to-surface mapping system," IEEE Trans. Geoscience and Remote Sensing, vol. 42, no. 4, pp. 754–763, 2004.
- [133] C. P. Davis, W. C. Chew, W. W. Tucker, and P. R. Atkins, "A null-field method for estimating underground position," *IEEE Trans. Geoscience* and Remote Sensing, vol. 46, no. 11, pp. 3731–3738, 2008.
- [134] M. Stojanovic and J. Preisig, "Underwater acoustic communication channels: Propagation models and statistical characterization," *IEEE Communications Magazine*, vol. 47, no. 1, pp. 84–89, 2009.
- [135] I. F. Akyildiz, P. Wang, and Z. Sun, "Realizing underwater communication through magnetic induction," *IEEE Communications Magazine*, vol. 53, no. 11, pp. 42–48, 2015.
- [136] X. Che et al., "Re-evaluation of rf electromagnetic communication in underwater sensor networks," *IEEE Communications Magazine*, vol. 48, no. 12, pp. 143–151, 2010.
- [137] L. Lanbo, Z. Shengli, and C. Jun-Hong, "Prospects and problems of wireless communication for underwater sensor networks," Wireless Communications and Mobile Computing, vol. 8, no. 8, pp. 977–994, 2008
- [138] M. C. Domingo, "Magnetic induction for underwater wireless communication networks," *IEEE Transactions on Antennas and Propagation*, vol. 60, no. 6, pp. 2929–2939, June 2012.
- [139] J. Park and P. P. Mercier, "Magnetic human body communication," in 2015 37th Annual International Conference of the IEEE Engineering in Medicine and Biology Society (EMBC), 2015, pp. 1841–1844.
- [140] B. Kibret, M. Seyedi, D. T. H. Lai, and M. Faulkner, "Investigation of galvanic-coupled intrabody communication using the human body circuit model," *IEEE Journal of Biomedical and Health Informatics*, vol. 18, no. 4, pp. 1196–1206, 2014.

- [141] D. Das, S. Maity, B. Chatterjee, and S. Sen, "Enabling covert body area network using electro-quasistatic human body communication," *Scientific reports*, vol. 9, no. 1, pp. 1–14, 2019.
- [142] K. Agarwal, R. Jegadeesan, Y. Guo, and N. V. Thakor, "Wireless power transfer strategies for implantable bioelectronics," *IEEE Reviews in Biomedical Engineering*, vol. 10, pp. 136–161, 2017.
- [143] https://www.cisco.com/c/dam/en/us/solutions/collateral/executive-perspectives/executive-perspectives/ccer_retail_global.pdf.
- [144] https://www.amazon.com/b?node=16008589011.
- [145] https://www.youtube.com/watch?v=BtXe1_6WY7k.
- [146] "Near-field magnetic induction (nfmi) technology for hearables and more," http://myemail.constantcontact.com/The-Audio-Voice-172--NFMI--Borbely-Hybrid-Headphone-Amp--Radian-Beryllium.html?soid=1104292817535&aid=TljcjgS7EGU.
- [147] V. J. R. B. GmbH), "Methods for robust wireless communication for nodes located in vehicles," Patent US9 363 685B2, 2016. [Online]. Available: https://patents.google.com/patent/US9363685B2/en
- [148] V. Jain, L. Venkatraman, and T. H. R. B. GmbH), "Magnetic field communication arrangement and method for a tractor-trailer," Patent US9 354 617B2, 2016. [Online]. Available: https://patents.google.com/ patent/US9354617B2/en
- [149] V. Jain, L. Venkatraman, and T. H. R. B. GmbH), "Magnetic field communication arrangement and method," Patent US9 256 212B2, 2016. [Online]. Available: https://patents.google.com/ patent/US9256212B2/en
- [150] A. R. Moghimi, H. Tsai, C. U. Saraydar, and O. K. Tonguz, "Characterizing intra-car wireless channels," *IEEE Transactions on Vehicular Technology*, vol. 58, no. 9, pp. 5299–5305, 2009.
- [151] E. Firmansyah, L. Grezelda, and Iswandi, "Rssi based analysis of bluetooth implementation for intra-car sensor monitoring," in *ICITEE*, 2014, pp. 1–5.
- [152] "Epson invests in rubee asset-tracking rfid tech," https://archive.eetasia.com/www.eetasia.com/ART_8800463942_499488_ NT 2d961d56.HTM.
- [153] "Automating the armory: New weapons tracker successfully tested by u.s. naval forces," http://www.designfax.net/cms/dfx/opens/articleview-dfx.php?nid=4&bid=499&et=news&pn=01.
- [154] L. G. Chen and K. Kulovic, "Acoustic transducer as a near-field magnetic induction coil," Patent 20190349660, November, 2019. [Online]. Available: http://www.freepatentsonline.com/y2019/0349660.html
- [155] A. M. Fitzgerald, "The internet of disposable things will be made of paper and plastic sensors," *IEEE Spectrum*, Nov 2018.
- [156] A. Singh et al., "Paper based sensors: emerging themes and applications," Sensors, vol. 18, no. 9, p. 2838, 2018.
- [157] F. Mustafa and S. Andreescu, "Chemical and biological sensors for food-quality monitoring and smart packaging," *Foods*, vol. 7, no. 10, p. 168, 2018.
- [158] L. Xie et al., "Integration of f-mwcnt sensor and printed circuits on paper substrate," *IEEE Sensors Journal*, vol. 13, no. 10, pp. 3948–3956, 2013.
- [159] H. W. Choi, T. Zhou, M. Singh, and G. E. Jabbour, "Recent developments and directions in printed nanomaterials," *Nanoscale*, vol. 7, pp. 3338–3355, 2015.
- [160] G.-W. Huang et al., "Rapid laser printing of paper-based multilayer circuits," ACS Nano, vol. 10, no. 9, pp. 8895–8903, 2016.
- [161] T. Cheng et al., "Inkjet printed large-area flexible circuits: a simple methodology for optimizing the printing quality," Journal of Semiconductors, vol. 39, no. 1, p. 015001, 2018.
- [162] N. Tal, Y. Morag, and Y. Levron, "Magnetic induction antenna arrays for mimo and multiple-frequency communication systems," *Progress In Electromagnetics Research*, vol. 75, pp. 155–167, 2017.
- [163] H. J. Kim et al., "Near-field magnetic induction mimo communication using heterogeneous multipole loop antenna array for higher data rate transmission," *IEEE Transactions on Antennas and Propagation*, vol. 64, no. 5, pp. 1952–1962, May 2016.
- [164] S. Hwang, H.-J. Kim, K. T. Kim, and J.-W. Choi, "Testbed implementation of near-field magnetic mimo communication system using sdr," in *Antennas and Propagation (ISAP)*, 2016 International Symposium on. IEEE, 2016, pp. 610–611.
- [165] X. Tan, Z. Sun, and I. F. Akyildiz, "A testbed of magnetic inductionbased communication system for underground applications," CoRR, 2015.



Amitangshu Pal received the B.E. degree in computer science and engineering from Jadavpur University, in 2008, and the Ph.D. degree in electrical and computer engineering from The University of North Carolina at Charlotte, in 2013. He was a Postdoctoral Scholar with Temple University, where he is currently an Assistant Professor with the Computer and Information Science Department. He has published over 50 papers in premier networking journals (e.g. ACM TOSN, ACM TOIT, IEEE IoTJ, IEEE Access) and conferences (e.g. ICCCN, LCN, WoWMoM,

Globecom, CCNC, WCNC). His current research interests include wireless sensor networks, reconfigurable optical networks, smart health-care, cyber-physical systems, mobile and pervasive computing, and cellular networks.



Krishna Kant was a Research Professor with George Mason University, and has served as the Program Director of the Computer, Information Science and Engineering Directorate, National Science Foundation (NSF), from 2008 to 2013.At NSF, he was also instrumental in the development and running of NSF wide sustainability initiative called SEES (science, engineering and education for sustainability). He has also served at Northwestern University, Penn State University, Bell Labs, Bellcore, and Intel, and carries a combined 34 years of experience in

academia, industry, and government. He is currently a Professor with Temple University, Philadelphia, PA, USA. His current areas of research include sustainability and energy efficiency in data centers, configuration robustness and security, and application of computing technologies to larger sustainability problems. He has published in a wide variety of areas in computer science, has authored a graduate textbook on performance modeling of computer systems, and has co-edited two books on infrastructure and cloud computing security. He is a Fellow of the IEEE.